

In the Name of God

Different types of Magnetic Nano-Particles and Optimization of Their Properties for Medical Applications

Presented by:
Hooman Shokrollahi

Electroceramics Group,
Materials Science and Engineering Dept.,
Shiraz University of Technology

E.mail: shokrollahi@sutech.ac.ir

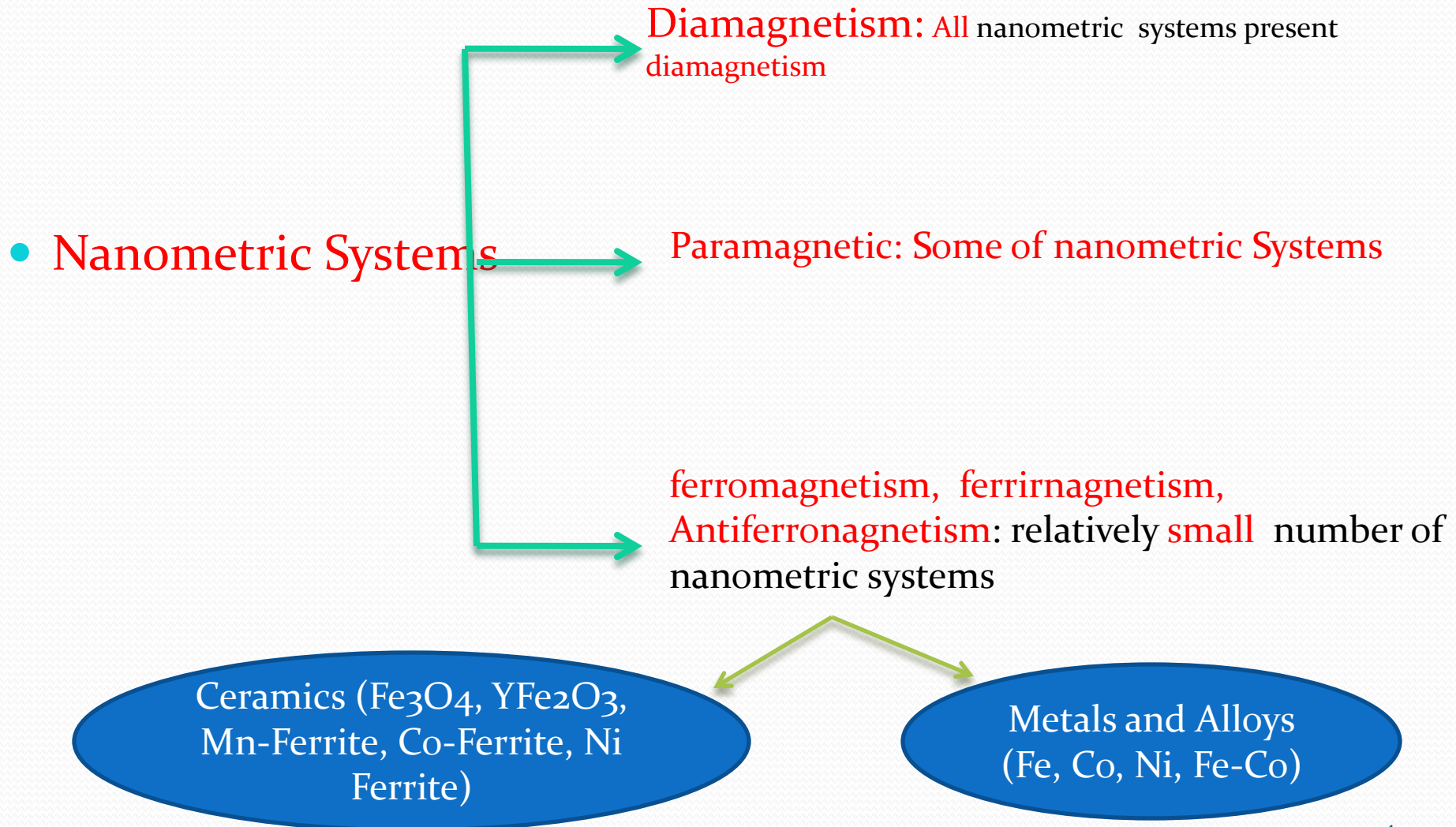
Presentation Topics

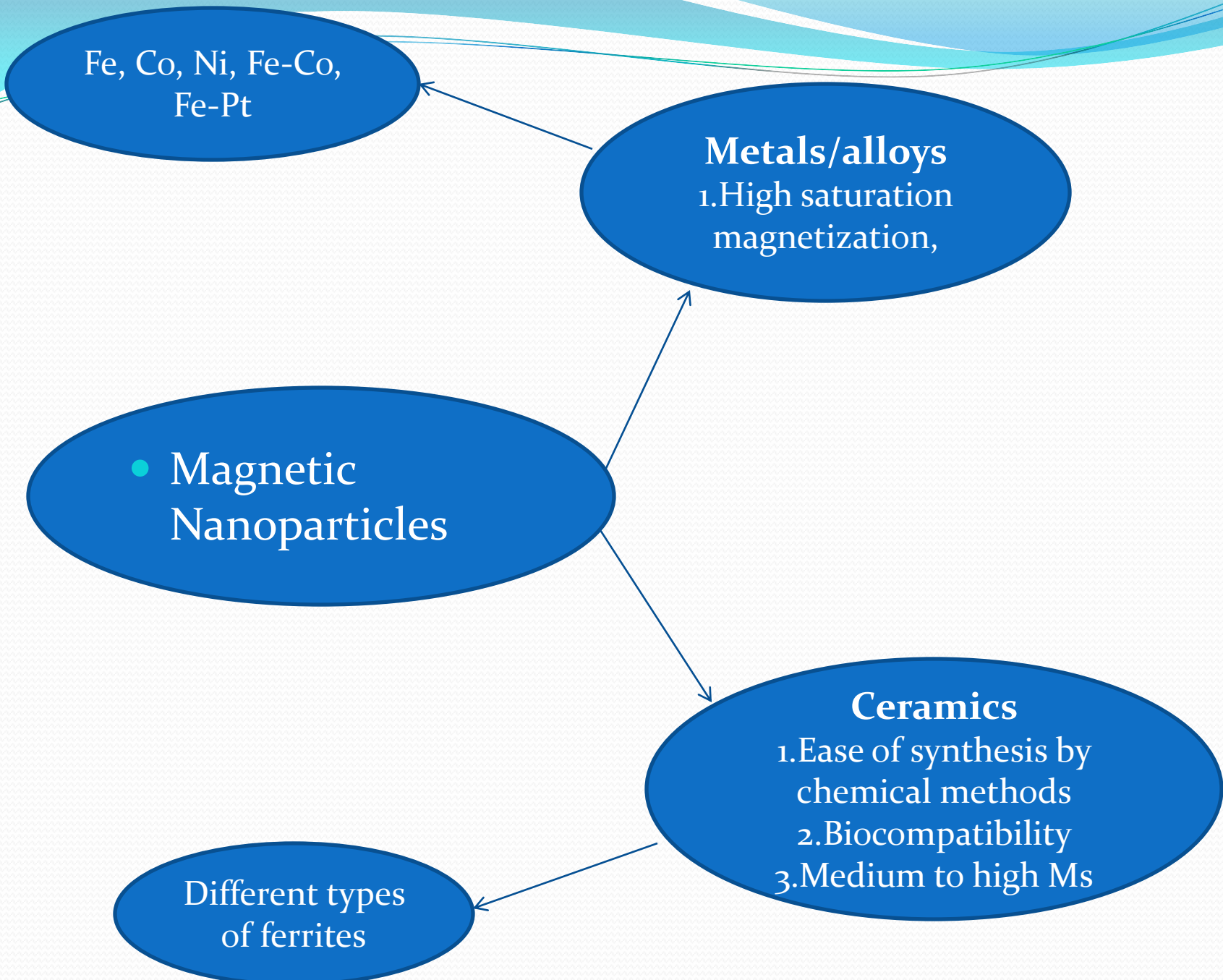
- 1. Magnetic Nano-Particles (MNPs)
- 2. Effective Parameters on MNPs Properties
- 3. Medical Applications

1. Magnetic Nano-Particles (MNPs)

Magnetic Nano-Particles

Magnetic properties of ultrafine particles are determined by their nanostructure





Fe, Co, Ni, Fe-Co,
Fe-Pt

Metals/alloys
1.High saturation magnetization,

• **Magnetic Nanoparticles**

Ceramics
1.Ease of synthesis by chemical methods
2.Biocompatibility
3.Medium to high Ms

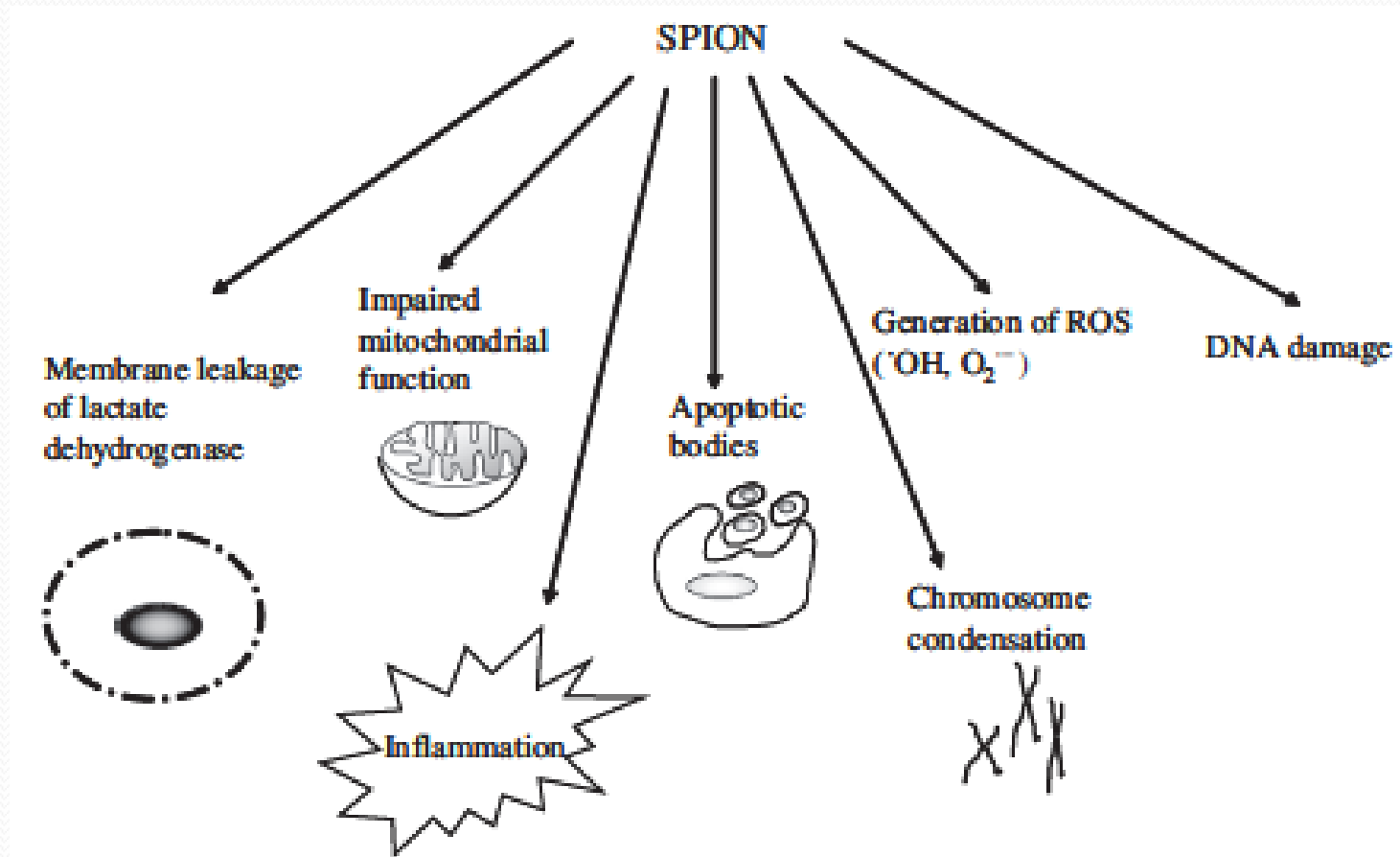
Different types of ferrites

Cellular toxicity induced by SPION



Institute of
Life Science
Wales
UK

Gareth J.S.
Jenkins



Nanoparticles

1. Ultrafine size
2. Surface condition (surface chemistry)
3. Magnetic Properties
4. Shape
5.

MNPs:

Limitations and advantages

- 1. The nature and magnetic state of the surface, and the different types of anisotropies in magnetic particles need to be explained. Although some of the developed theories are relatively complex, they do not explain the experimental values observed by the hysteresis behavior of many of the real particle systems.
- 2. Another problem of great interest to be clarified involves the interactions between particles.
- 3. The nanometric size is ideal for the study of magnetic phenomena at the mesoscopic or microscopic level (fundamental studies)

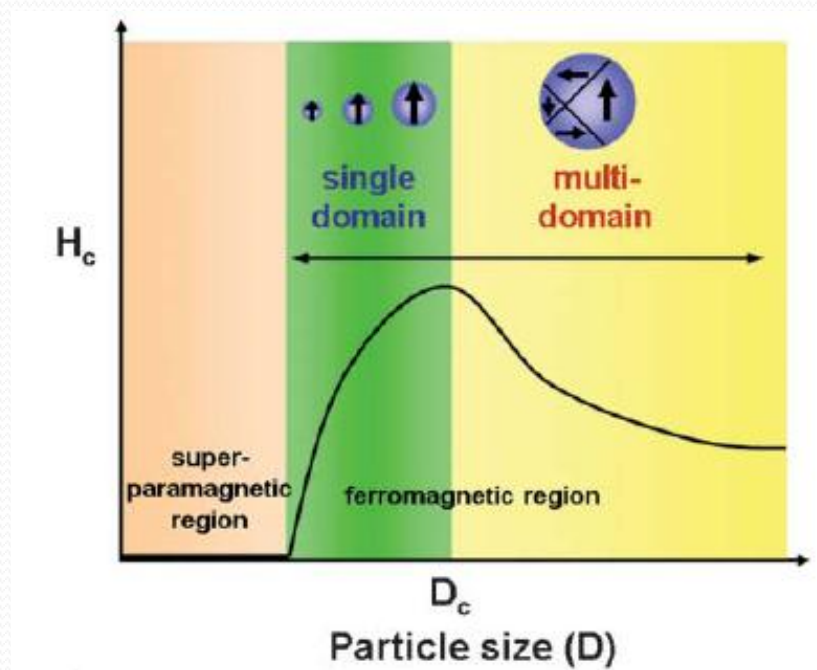
- Ultrafine particles

- 1. Multi-domain

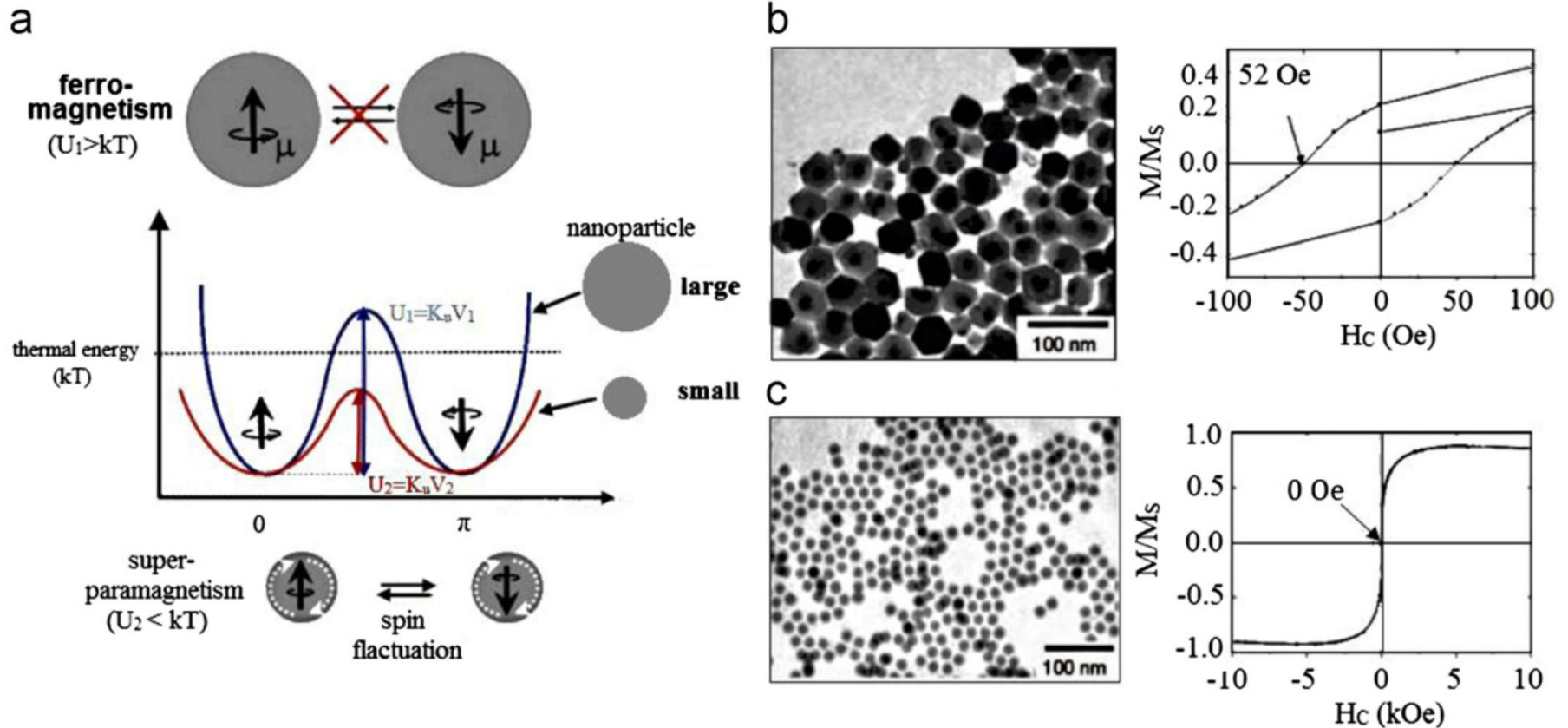
- 2. Single-domain: depends on the composition, structure and shape of the particles.

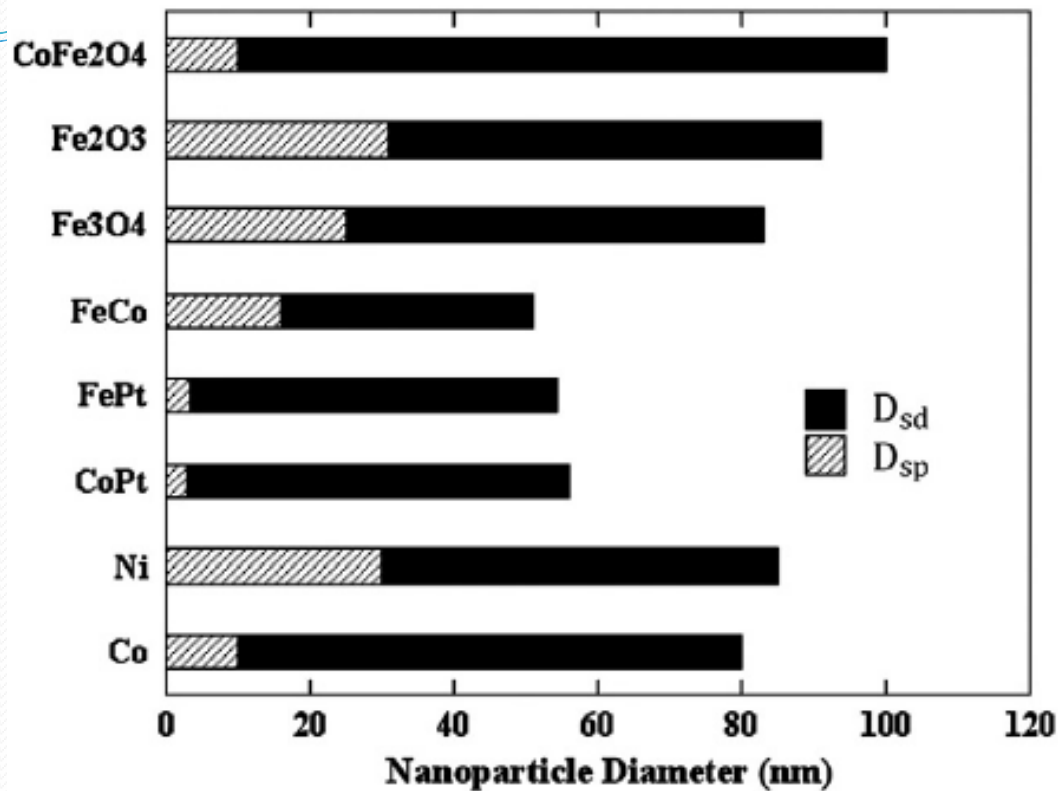
- 3. Superparamagnetic: medical Applications

- 4. Clusters



- b and c depicts the size dependent transition of iron oxide nanoparticles from superparamagnetic to ferromagnetic. Also they show TEM images and hysteresis loops of (b) 55nm and (c) 12nm sized iron oxide nanoparticles.





- Critical sizes for **superparamagnetic and single domain size** as anticancer agents in locoregional tumor therapy, a measurement time of 100 s is assumed in all
 - cases.

Nanoscale magnetic particles: synthesis, structure and dynamics

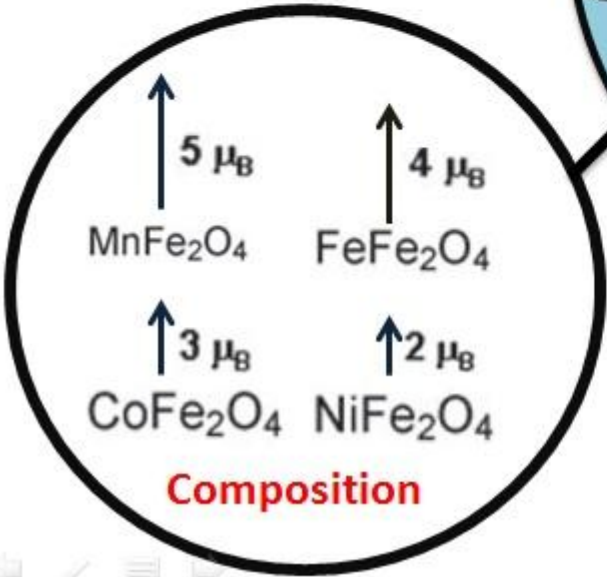
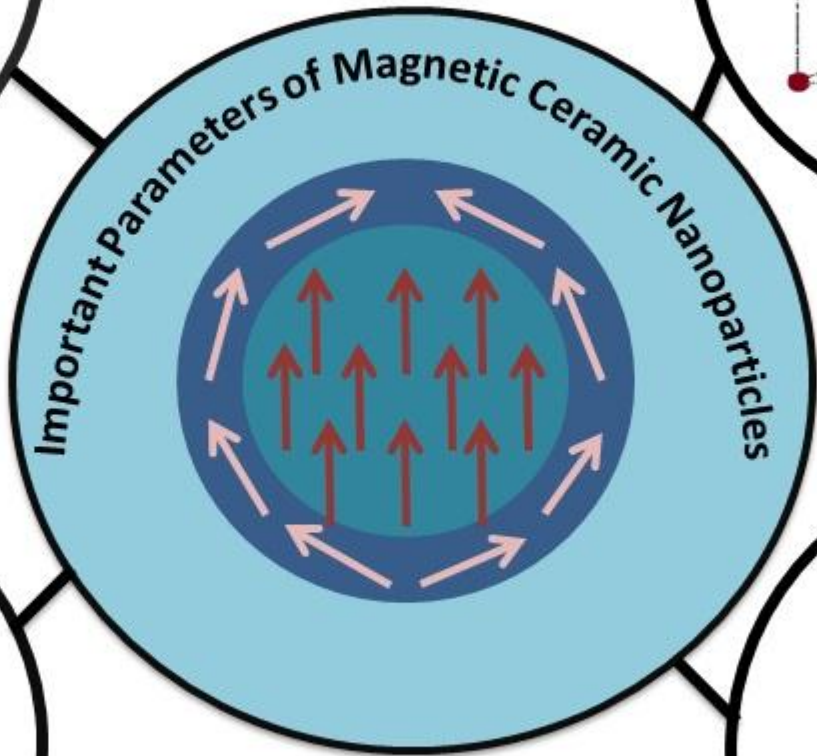
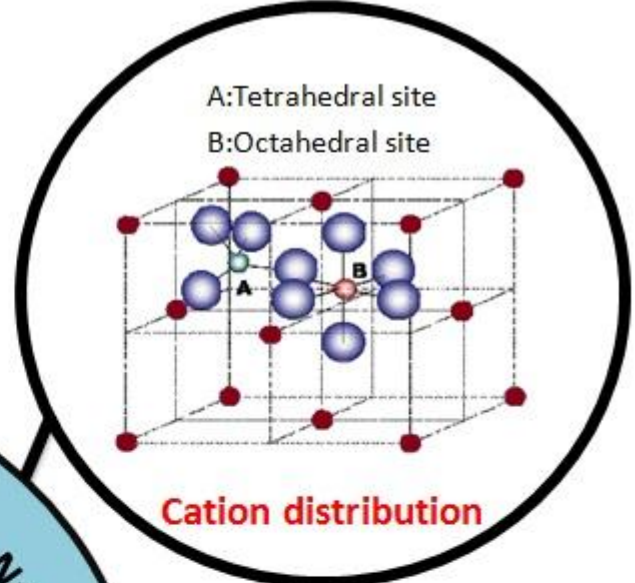
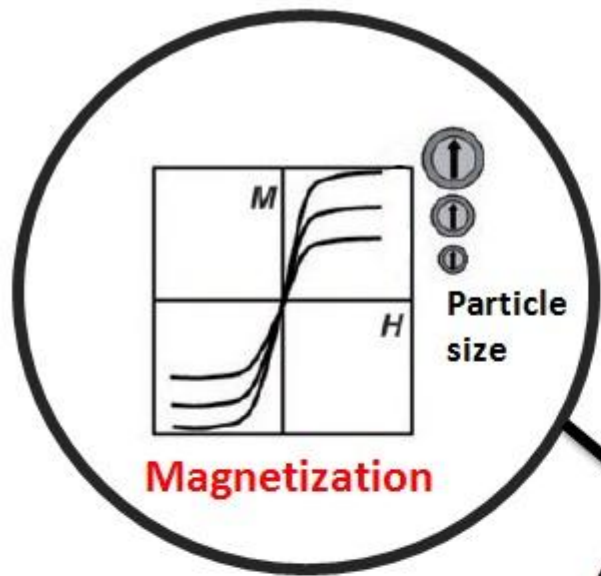
M Arturo López-Quintela* and José Rivas†

In recent years, new synthetic routes, which include wet techniques and synthesis in confined geometries, have been developed for the preparation of nanoscale magnetic particles. The shape of the particles obtained is usually smooth and rounded all over, due to the influence of the surface energy. The final shape, however, depends on the preparation method and is much influenced by the substrate used, as this may stress and deform the particles in order that

phenomena which range from the limits of quantum mechanics to classical phenomena [5**]. For these reasons, the development of new general methods for obtaining ultrafine particles that are simple and produce reliable results, as well as the characterization and study of the physical and chemical properties of these systems hold a great importance.

2. Effective Parameters on MNPs Properties

- a. Particle Size
- b. Chemical Composition
- c. Cation Distribution
- d. Cation Environment
- e. Synthesis Method
- f. Particle shape

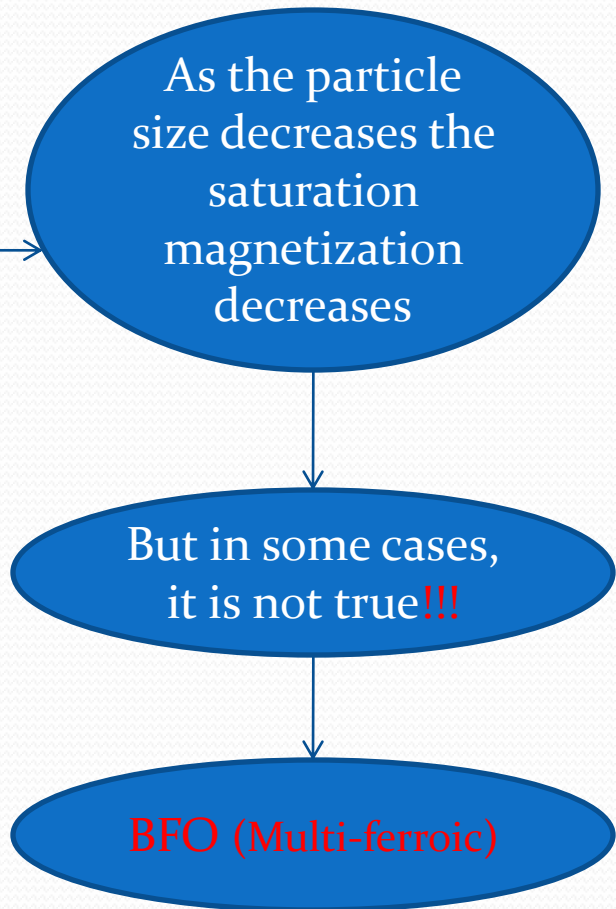
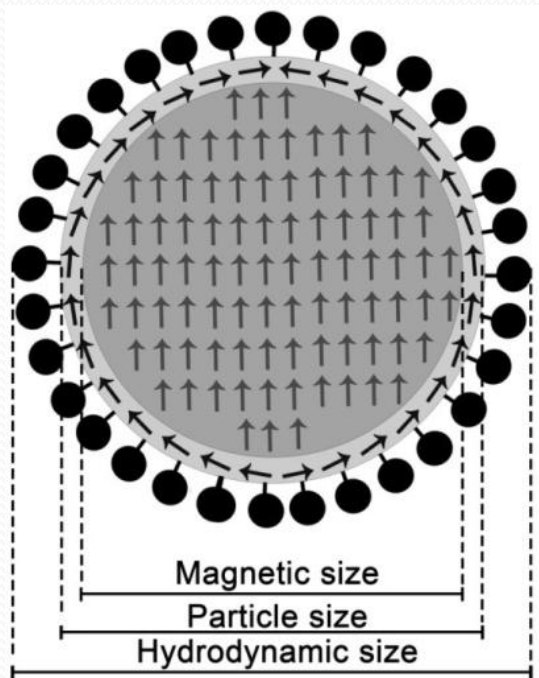


Microemulsion
Coprecipitation
Thermal decomposition
Hydrothermal

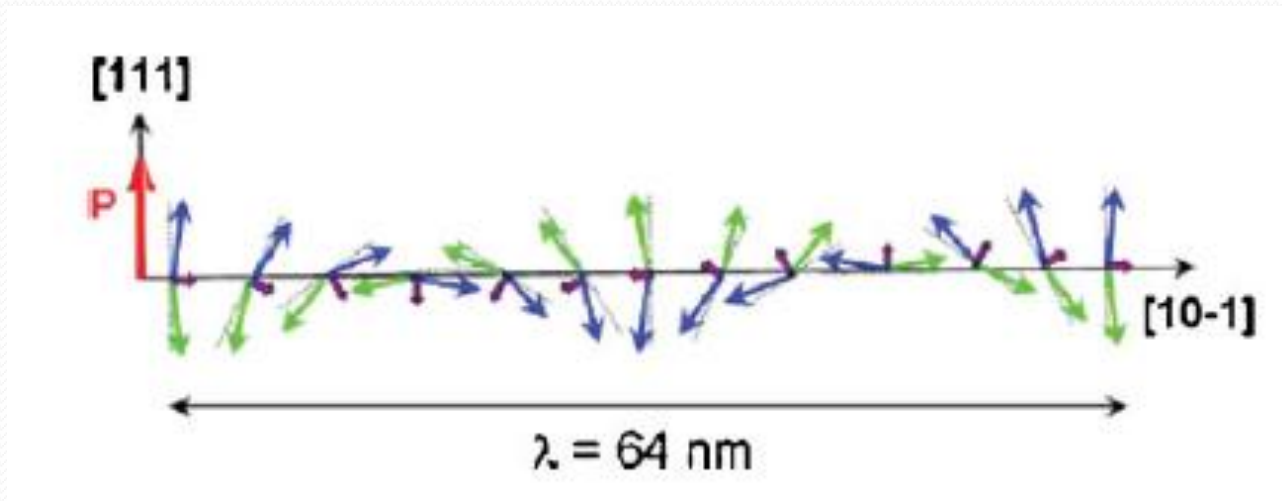
Diagram illustrating the synthetic methods for magnetic ceramic nanoparticles, showing a beaker with bubbles and a magnetic stirrer.

Synthetic methods

a. Particle size

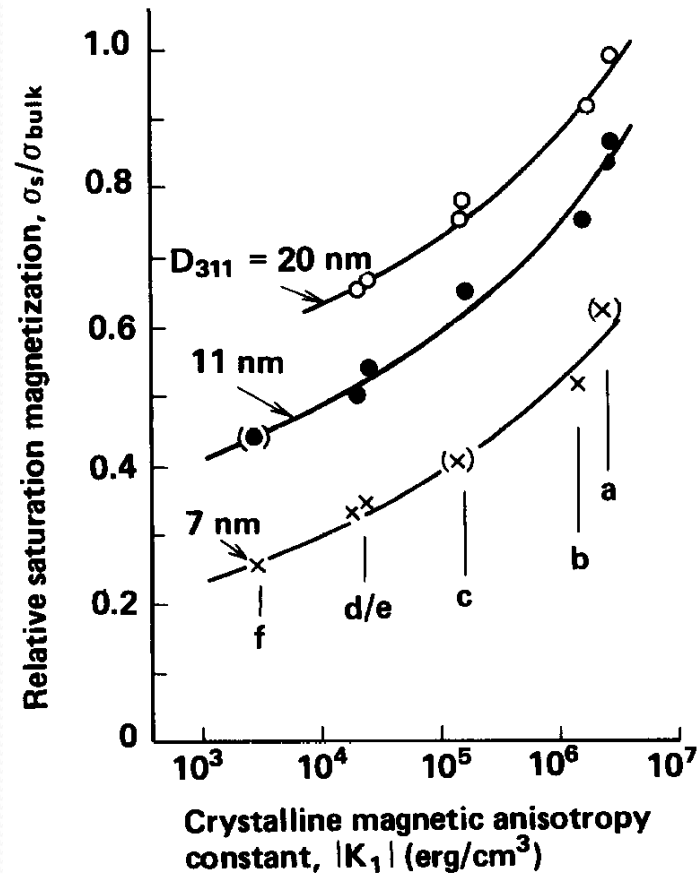
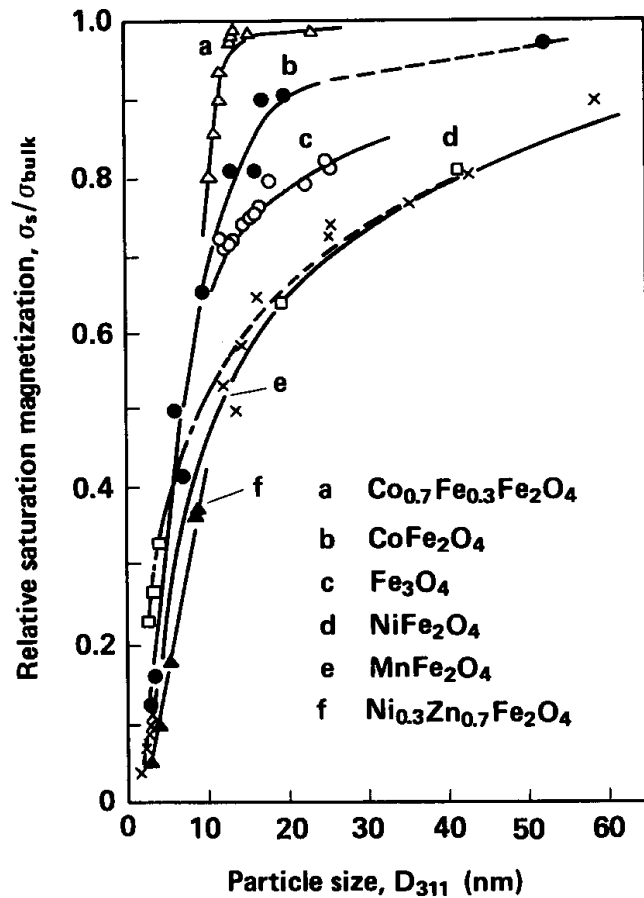


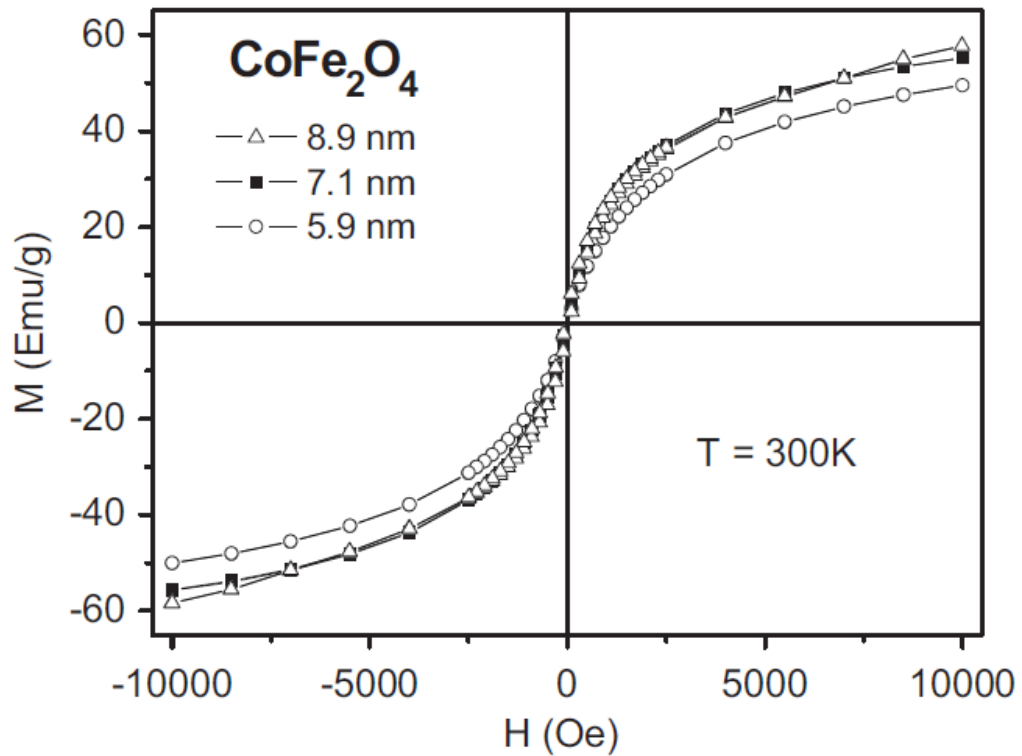
- Hydrodynamic size: medical applications
 - Particle size: Magnetic studies



- Schematic representation of the spin cycloid. The canted antiferromagnetic
- spins (blue and green arrows) give rise to a net magnetic moment (purple arrows) that is spatially averaged out to zero due to the cycloidal rotation. The spins are contained within the plane defined by the polarization vector (red) and the cycloidal propagation vector (black).

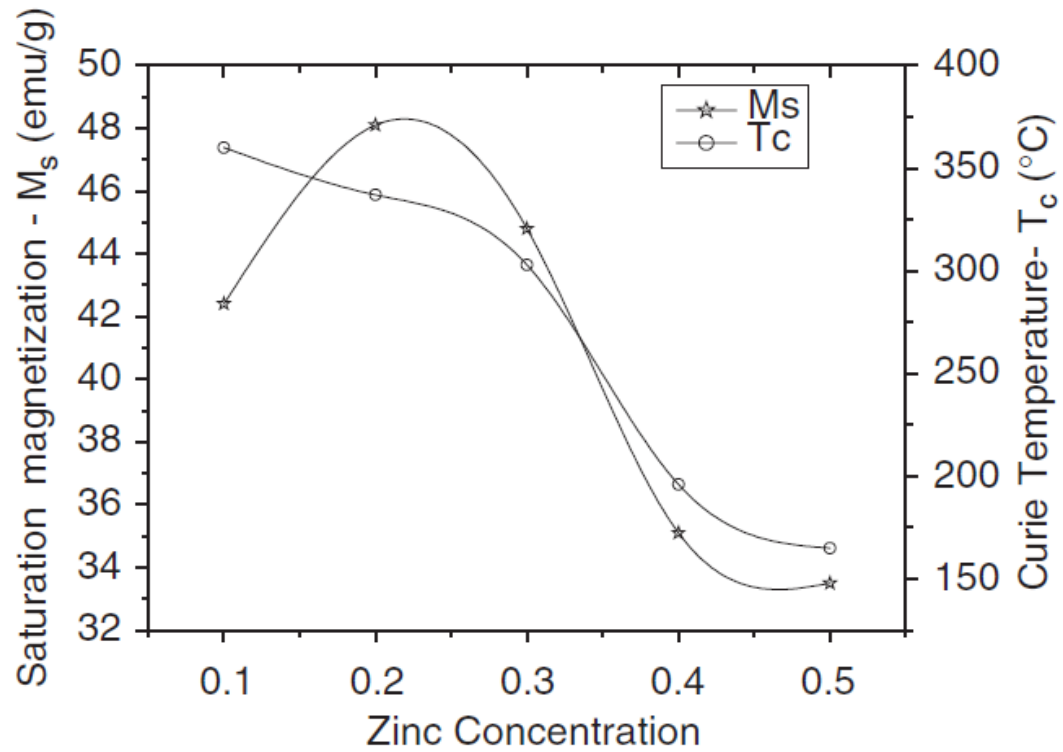
Toshihiko SATO, 1987, Japan

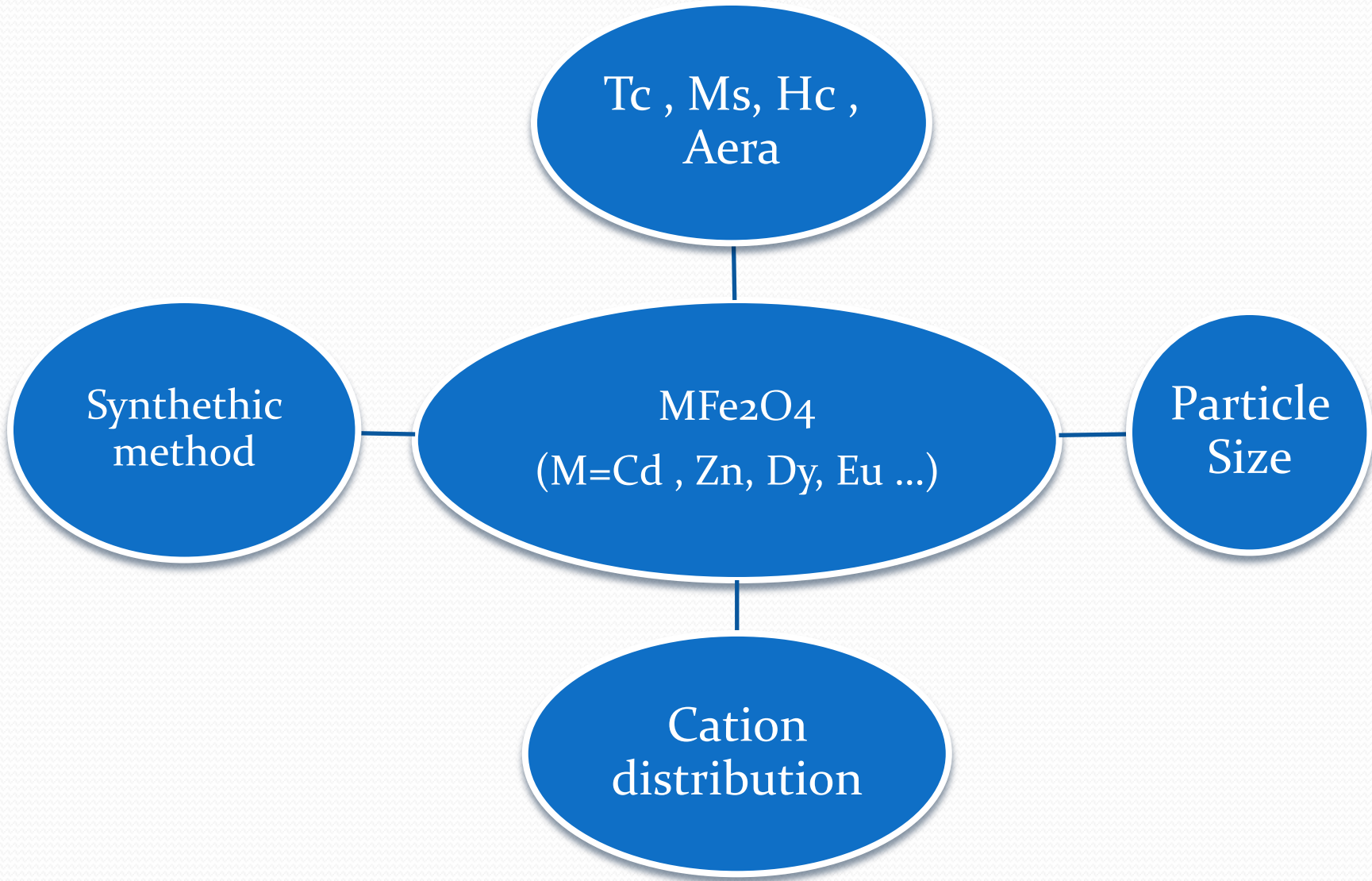




b. Chemical Composition

Ferrite	Spinel type	Chemical formula	M_s emu/g	D_C (nm)	D_{SP} (nm)
$CoFe_2O_4$	Inversed spinel	$Fe^{3+}[Co^{2+}Fe^{3+}]O_4^{2-}$	80-94	70	14
$NiFe_2O_4$	Inversed spinel	$Fe^{3+}[Ni^{2+}Fe^{3+}]O_4^{2-}$	56	100	28
Fe_3O_4	Inversed spinel	$Fe^{3+}[Fe^{2+}Fe^{3+}]O_4^{2-}$	90-100	128	25
$MnFe_2O_4$	Mixed spinel	$Me_{1-\delta}^{2+}Fe_{\delta}^{3+}[Me_{\delta}^{2+}Fe_{2-\delta}^{3+}]O_4^{2-}$	80	128	25

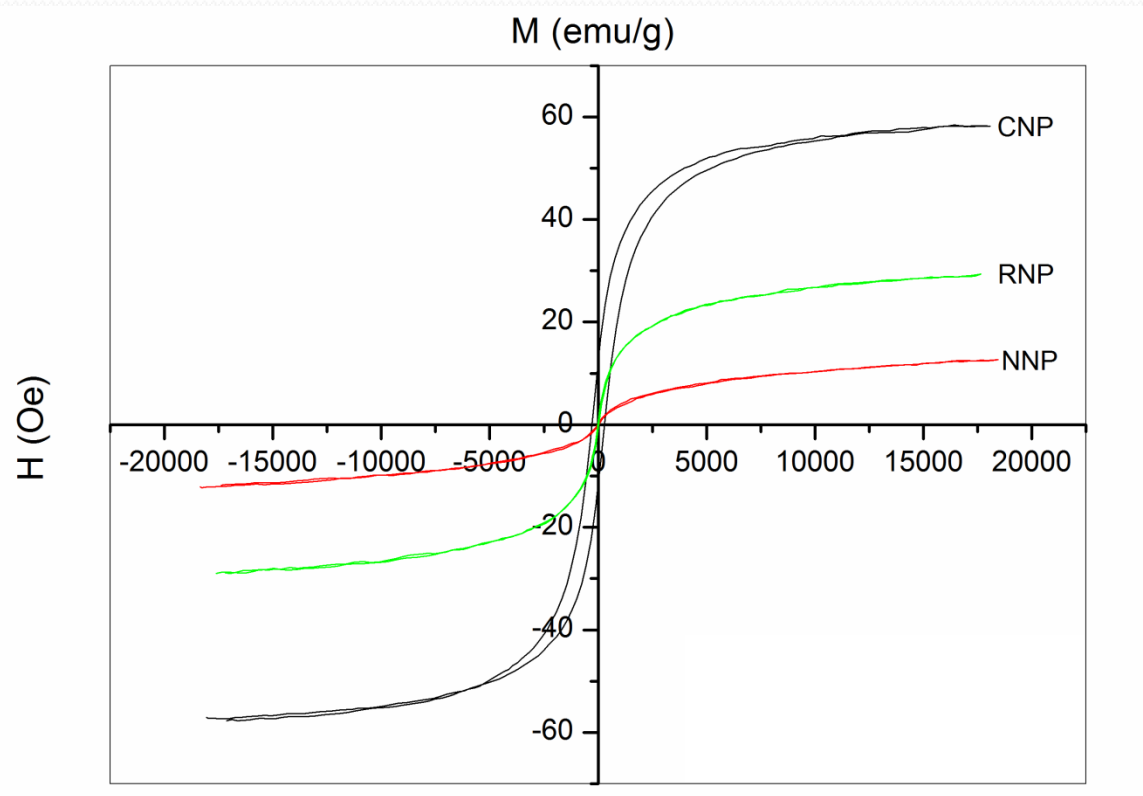




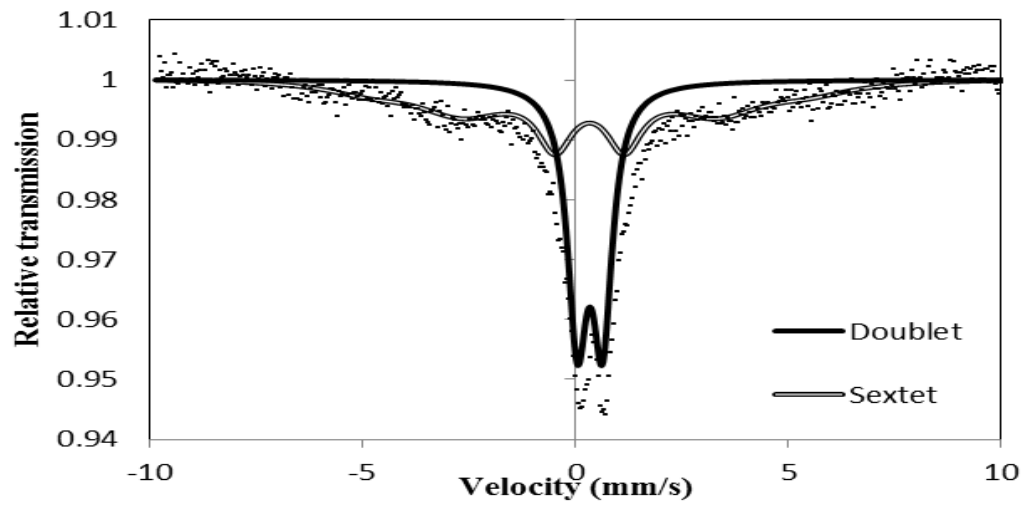
C. Cation Distribution

Synthesis method	Formula	a_{exp} (nm)	a_{th} (nm)	D (nm)	U^{3m} (nm)	u (nm)
CNP	$[Co_{0.165}^{2+} Fe_{0.835}^{3+}]^A [Co_{0.835}^{2+} Fe_{1.165}^{3+}]^B O_4$	0.84028	0.84021	11.70	0.02614	0.038305
NNP	$[Co_{0.010}^{2+} Fe_{0.990}^{3+}]^A [Co_{0.990}^{2+} Fe_{1.010}^{3+}]^B O_4$	0.83913	0.83989	5.58	0.02603	0.038322
RNP	$[Co_{0.124}^{2+} Fe_{0.876}^{3+}]^A [Co_{0.876}^{2+} Fe_{1.124}^{3+}]^B O_4$	0.84009	0.84012	7.63	0.02611	0.038315

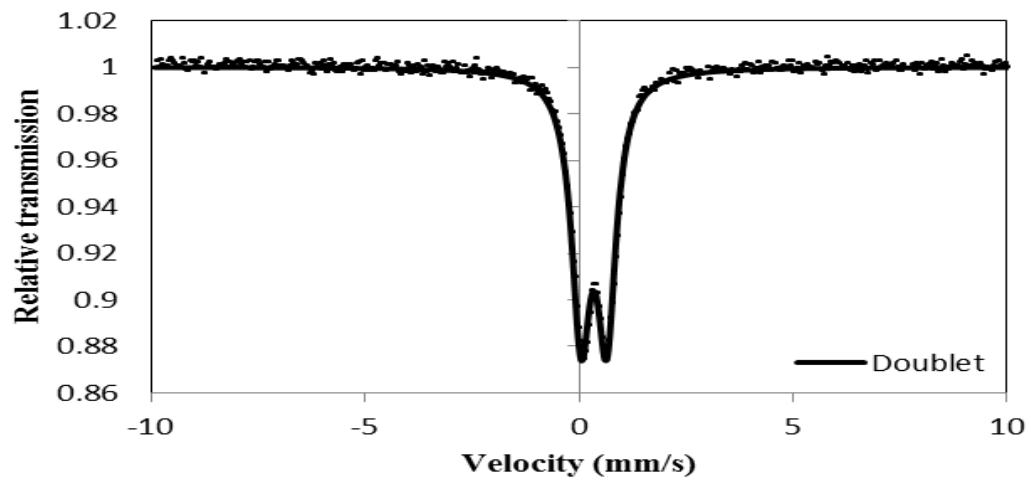
Synthesis method	M_s (emu/g)	H_c (Oe)	M_r (emu/g)	H_{max} (kOe)	t_{shell} (nm)
CNP	58.4	286.0	12.45	18.0	0.74
NNP	12.6	23.7	0.17	18.4	0.80
RNP	29.4	25.2	0.84	17.6	0.87



Samples	D (nm)	a (nm)	site occupancy			atomic coordinates (x=y=z)			R _{wp} (%)	R _p (%)	χ ² (%)
			Co/Mn /Zn	Fe	O	Co/Zn	Fe	O			
(M0) Co _{0.5} Zn _{0.5} Fe ₂ O ₄	9.8	0.8413	0.878	0.899	1.000	0.0000	0.6250	0.3832	7.00	5.20	1.05
(M1) Co _{0.4} Mn _{0.1} Zn _{0.5} Fe ₂ O ₄	7.8	0.8424	0.831	0.946	1.000	0.0000	0.6250	0.3886	8.25	6.55	2.14
(M2) Co _{0.3} Mn _{0.2} Zn _{0.5} Fe ₂ O ₄	7.6	0.8433	0.886	0.986	1.000	0.0000	0.6250	0.3887	8.15	6.43	2.66
(M3) Co _{0.2} Mn _{0.3} Zn _{0.5} Fe ₂ O ₄	6.7	0.8436	0.860	0.929	1.000	0.0000	0.6250	0.3887	7.88	6.21	1.88
(M4) Co _{0.1} Mn _{0.4} Zn _{0.5} Fe ₂ O ₄	7.6	0.8440	0.865	0.980	1.000	0.0000	0.6250	0.3886	7.24	5.50	1.83
(M5) Mn _{0.5} Zn _{0.5} Fe ₂ O ₄	5.0	0.8433	1.000	0.869	0.825	0.0000	0.6250	0.3842	6.52	5.03	1.12



M0

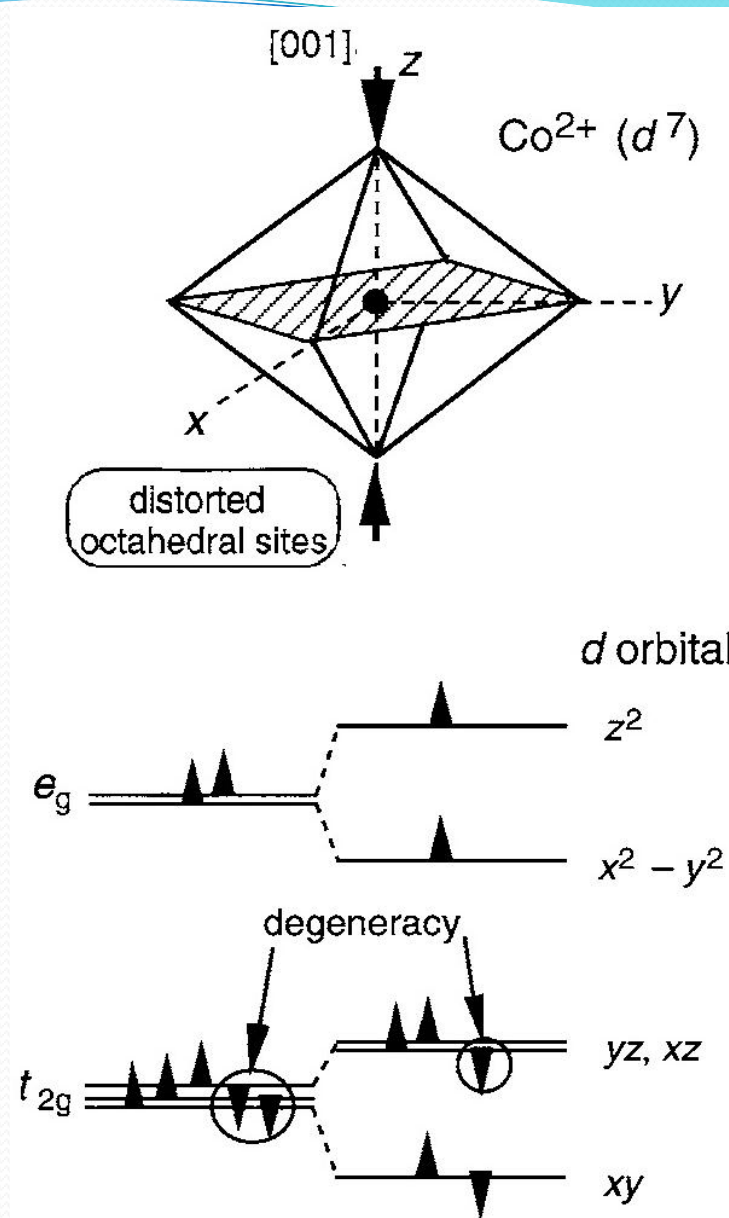


• M5

d.Cation Environment

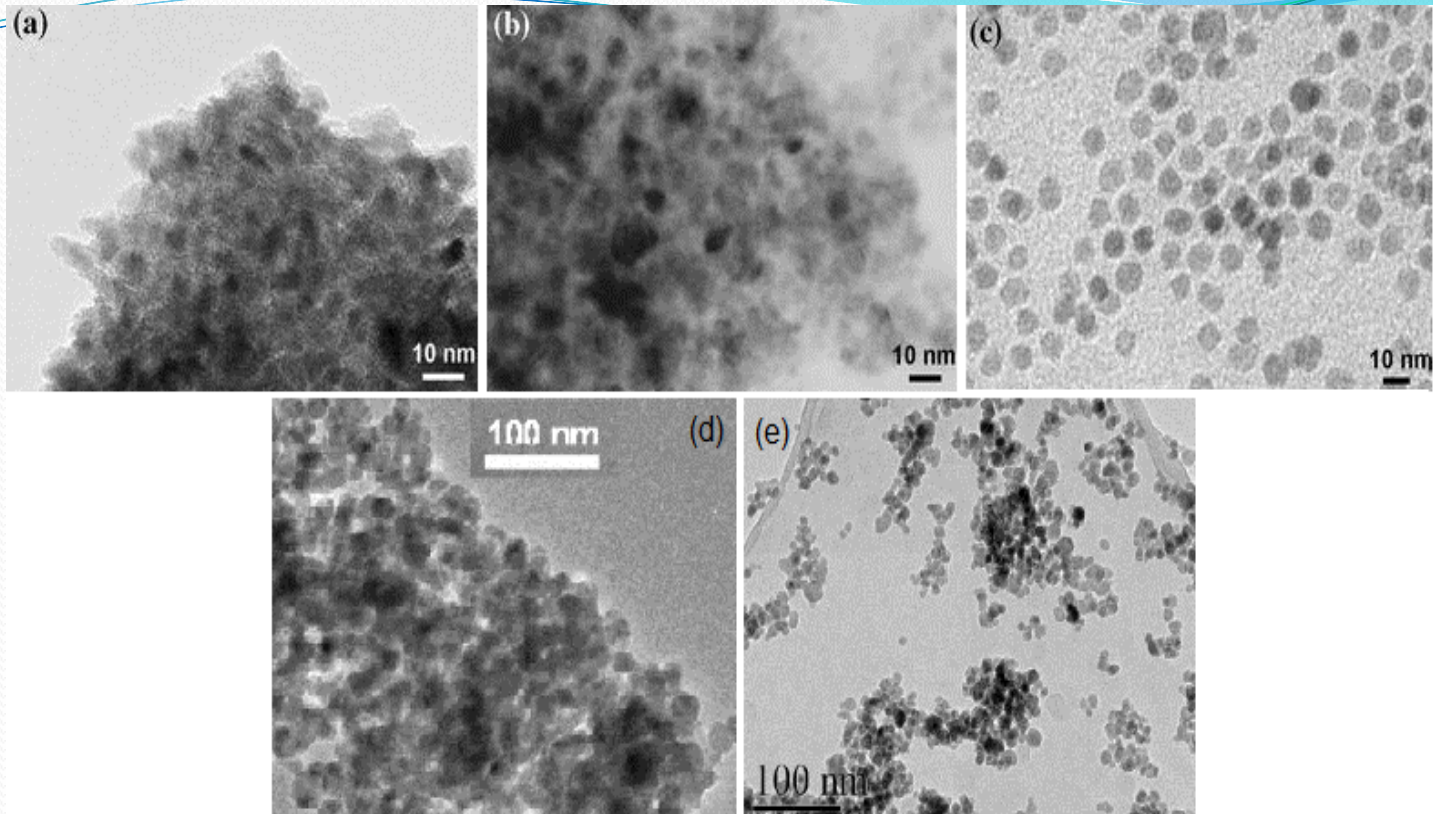
TABLE 6.2 Level Fillings and Degeneracies for Selected Transition Metal Ions^a

Ion	Electron Configuration	Octahedral			Tetrahedral		
		Orbital Configuration	$\langle L_z \rangle$	Degeneracy	Orbital Configuration	$\langle L_z \rangle$	Degeneracy
Cr ²⁺	3d ⁴	$t_{2g}^3 e_g^1$	≠ 0	2	$e_g^2 t_{2g}^2$	≠ 0	3
Mn ²⁺	3d ⁵	$t_{2g}^3 e_g^2$	0	0		0	0
Fe ³⁺							
Fe ²⁺	3d ⁶	$t_{2g}^4 e_g^2$	≠ 0	3	$e_g^3 t_{2g}^3$	≠ 0	2
Co ²⁺	3d ⁷	$t_{2g}^5 e_g^2$	≠ 0	3	$e_g^4 t_{2g}^3$	0	1
Ni ²⁺	3d ⁸	$t_{2g}^6 e_g^2$	0	0	$e_g^4 t_{2g}^4$	≠ 0	3
Cu ²⁺	3d ⁹	$t_{2g}^6 e_g^3$	≠ 0	2	$e_g^5 t_{2g}^4$	≠ 0	3

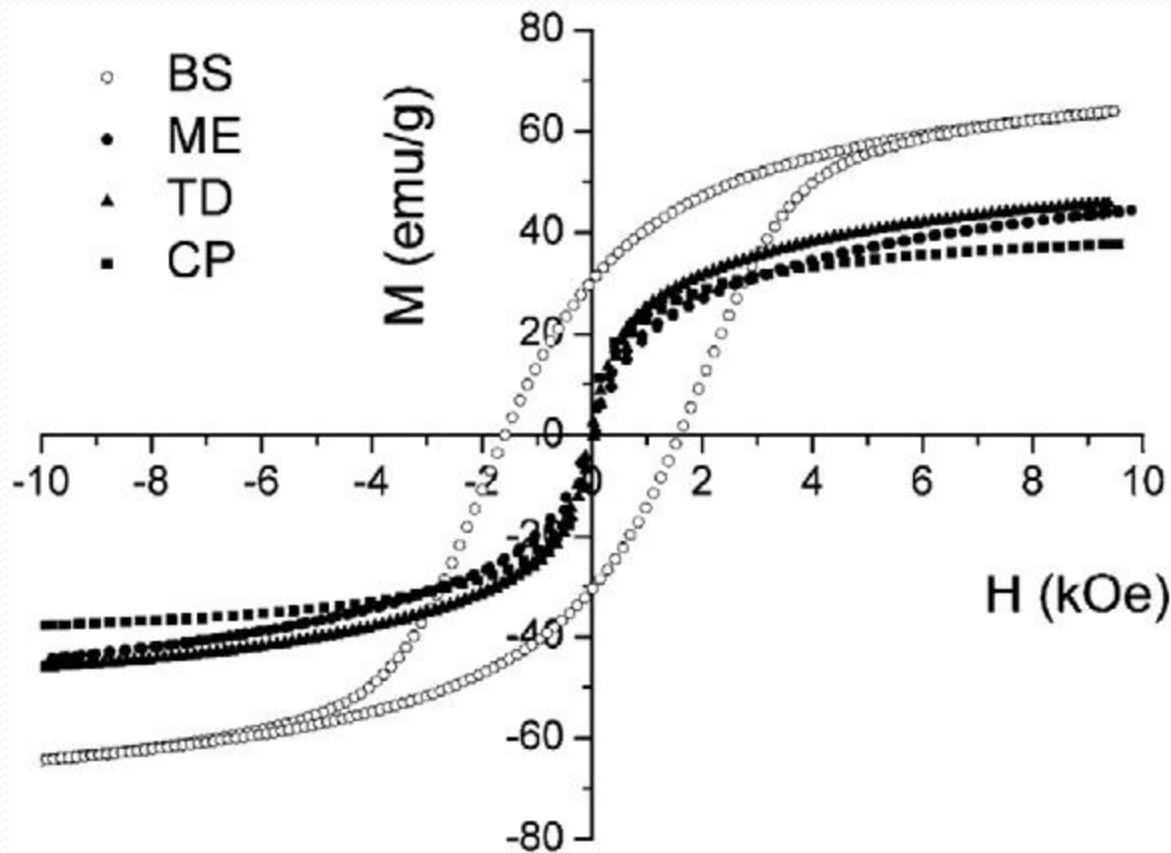


e. Synthesis method

Synthetic method	Synthesis	Reaction temp. [°C]	Reaction period	Solvent	Surface-capping agents	Size distribution	Shape control	Yield
co-precipitation	very simple, ambient conditions	20–90	minutes	water	needed, added during or after reaction	relatively narrow	not good	high/ scalable
Thermal decomposition	Complicated, inert atmosphere	100–320	hours-days	Organic compound	needed, added during reaction	very narrow	very good	high/ scalable
microemulsion	Complicated, ambient conditions	20–50	hours	organic compound	needed, added during reaction	relatively narrow	good	low
hydrothermal synthesis	simple, high pressure	220	hours-days	water-ethanol	needed, added during reaction	very narrow	very good	medium



- TEM images of the Co-ferrite nanoparticles synthesis by (a) coprecipitation (b) microemulsion (c) thermal decomposition (d) sol-gel (e) hydrothermal



Room-temperature magnetization curves for the Co-ferrite nanoparticles CP, ME, and TD and standard BS. The co-precipitated nanoparticles (CP) were annealed at 600 °C for 15 h in an ambient air.

Effective Parameters (Wet Chemistry)

1. External Parameters: Temperature, pH, Concentration
2. Internal Parameters: Energy of formation, Entropy of formation, Electronic configuration, Binding energy

Samples	D (nm)	a (nm)	site occupancy			atomic coordinates (x=y=z)			R _{wp} (%)	R _p (%)	χ ² (%)
			Co/Mn/Zn	Fe	O	Co/Zn	Fe	O			
(M0) Co _{0.5} Zn _{0.5} Fe ₂ O ₄	9.8	0.8413	0.878	0.899	1.000	0.0000	0.6250	0.3832	7.00	5.20	1.05
(M1) Co _{0.4} Mn _{0.1} Zn _{0.5} Fe ₂ O ₄	7.8	0.8424	0.831	0.946	1.000	0.0000	0.6250	0.3886	8.25	6.55	2.14
(M2) Co _{0.3} Mn _{0.2} Zn _{0.5} Fe ₂ O ₄	7.6	0.8433	0.886	0.986	1.000	0.0000	0.6250	0.3887	8.15	6.43	2.66
(M3) Co _{0.2} Mn _{0.3} Zn _{0.5} Fe ₂ O ₄	6.7	0.8436	0.860	0.929	1.000	0.0000	0.6250	0.3887	7.88	6.21	1.88
(M4) Co _{0.1} Mn _{0.4} Zn _{0.5} Fe ₂ O ₄	7.6	0.8440	0.865	0.980	1.000	0.0000	0.6250	0.3886	7.24	5.50	1.83
(M5) Mn _{0.5} Zn _{0.5} Fe ₂ O ₄	5.0	0.8433	1.000	0.869	0.825	0.0000	0.6250	0.3842	6.52	5.03	1.12

- The general decrease in the particle size by the increase in Mn content may be explained by
 - (i) the electronic configuration of Co^{2+} ($3d^7$), and
 - (ii) its further tendency to interact with ligands and oxygen anions, as compared to Mn^{2+} ($3d^5$), which has a complete electronic configuration.
 - (iii) Furthermore, it is interesting to note that Zn^{2+} ions in the spinel structure have a very strong preference for tetrahedral sites and Co^{2+} ions have a similar strong preference for octahedral sites.
 - (iv) Also, Mn^{2+} ions have a stronger preference for the tetrahedral sites as compared to the octahedral sites. Thus the formation of Mn-ferrite is less favorable, so that generally, the grain size slightly decreases as the Mn content increases as a result of site preferences.

Chemical Reactions in Microemulsions: A Powerful Method to Obtain Ultrafine Particles

M. ARTURO LÓPEZ-QUINTELA¹ AND JOSÉ RIVAS

*University of Santiago de Compostela, Laboratory of Powder Technology, Dpts. of Physical Chemistry
and Applied Physics, E-15706 Santiago de Compostela, Spain*

JOURNAL OF COLLOID AND INTERFACE SCIENCE **158**, 446–451 (1993)

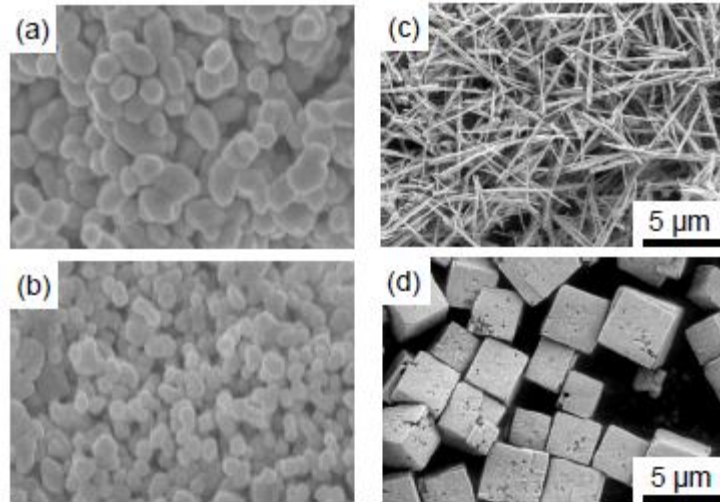
Hydrothermal Synthesis of Advanced Ceramic Powders

Wojciech L. Suchanek^{1, a} and Richard E. Riman^{2, b}

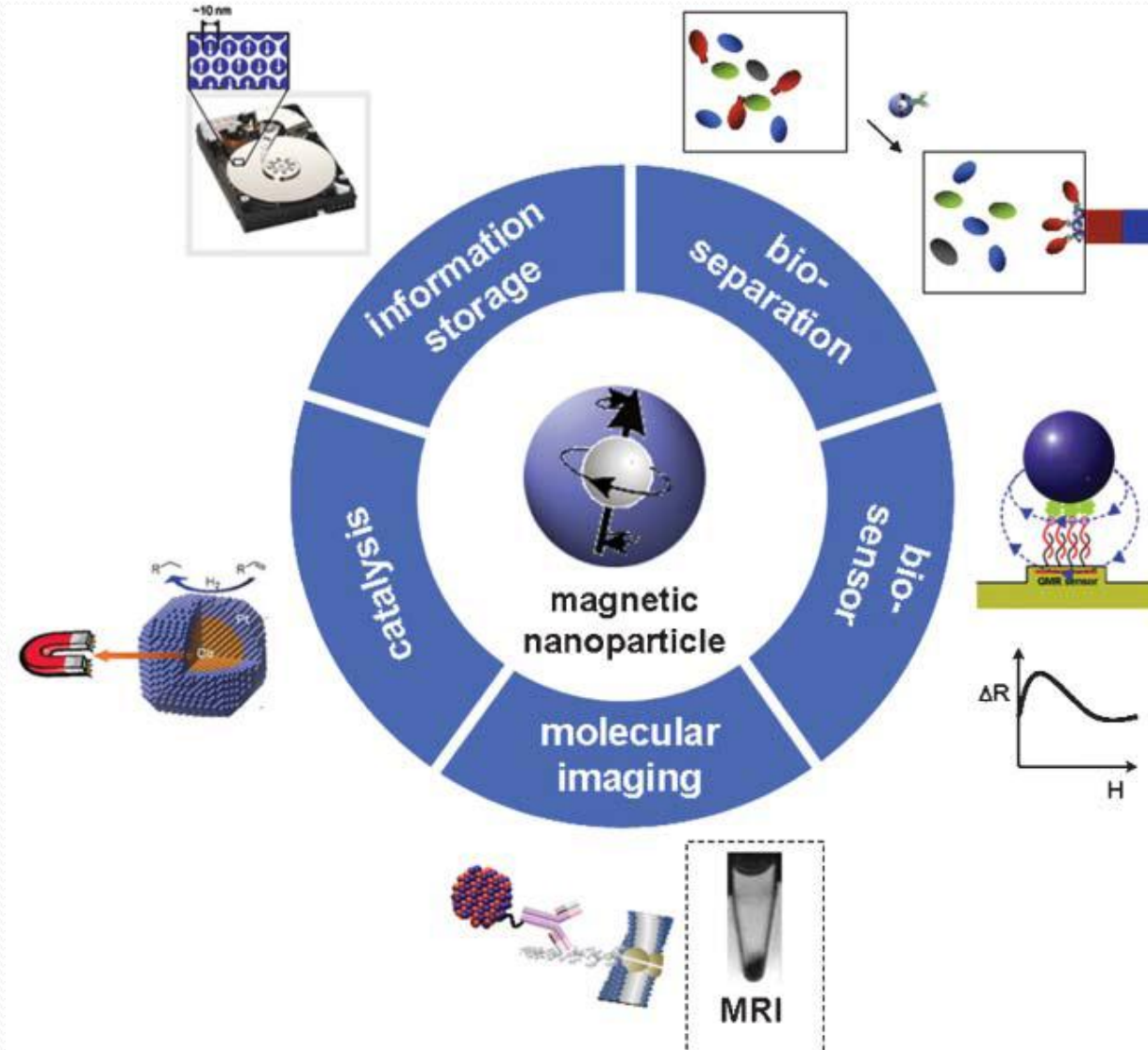
¹Sawyer Technical Materials, LLC, 35400 Lakeland Boulevard, Eastlake, OH 44095, USA

²Rutgers University, Department of Materials Science and Engineering, 607 Taylor Road, Piscataway, NJ 08855, USA

^awls@SawyerLLC.com, ^briman@email.rci.rutgers.edu



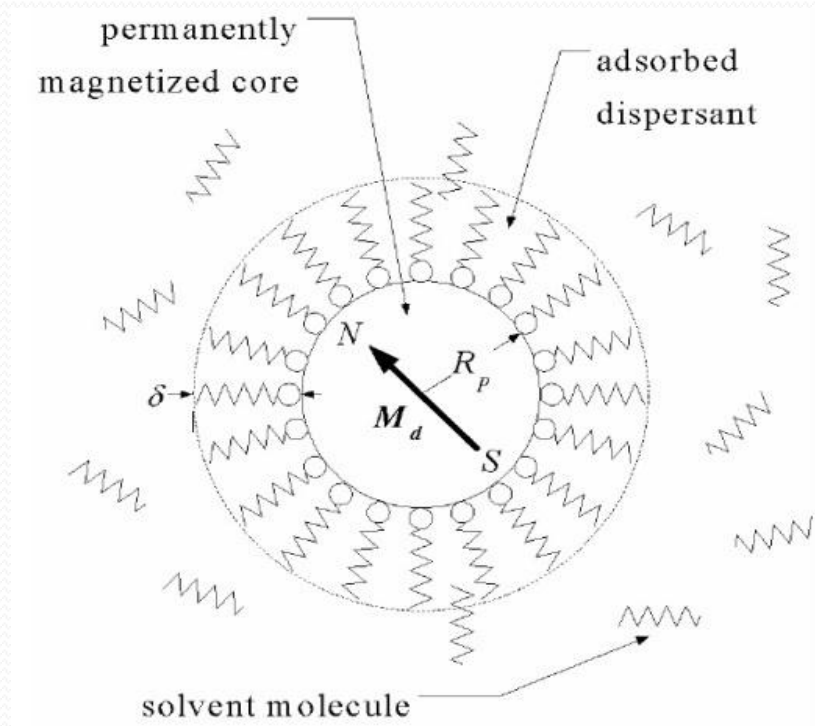
3. Magnetic Nano-particles Applications



Medical Applications

- Hyperthermia
 - MRI
 - Drug Targeting
-
- In medical applications the magnetic nanoparticles are used for *diagnostics and therapy*.

2. Hyperthermia



Interaction force	equation	Ferrofluid stability criteria	description	Particle type
Magnetic field energy	$ E_{\text{mag}} = \mu_0 M_0 V H$	$kT / \mu_0 M H V \geq 1$ $d \leq \left(\frac{6kT}{\pi \mu_0 M H} \right)^{1/2}$	(attractive)	uncoated particles
gravitational field	$E_{\text{grav}} = \Delta \rho V g h$	$\frac{\Delta \rho g L}{\mu_0 M H} \ll 1$	attractive	uncoated particles
dipole-dipole contact energy	$E_{\text{dip}} = \frac{\mu_0 M^2 V}{12}$	$\frac{12kT}{\mu_0 M^2 V} \geq 1$ $d \leq \left(\frac{72kT}{\pi \mu_0 M^2} \right)^{1/3}$	attractive	uncoated particles
dipole-dipole un-contact energy	$v(r_{ij}, \mu_i, \mu_j) = v_{\text{sr}}(r_{ij}) + \frac{1}{r_{ij}^3} \left[\mu_i \mu_j - \frac{3(\mu_i \cdot r_{ij})(\mu_j \cdot r_{ij})}{r_{ij}^2} \right]$	-	attractive	uncoated particles
Van der Waals	$E_{\text{vdw}} = -\frac{A}{6} \left[\frac{2}{l^2 + 4l} + \frac{2}{(l+2)^2} + \ln \left(\frac{l^2 + 4l}{(l+2)^2} \right) \right]$	thermal energy cannot re-disperse the particles being in contact and depends on the inter-particle distance	attractive	uncoated particles
Steric repulsion	-	It is much more short-ranged and operates at distances of the overlap of the surface layers	repulsive	coated particles

Different loss mechanisms under different average particle sizes.

Various conditions	$D > D_{SD}$	$D \sim D_{SD}^a$	$D_{SP}^b < D < D_{SD}$	$D \sim D_{SP}$	$D \leq D_{SP}^c$
Dominant loss mechanism/s	Hysteresis + Eddy current ^d + anomalous ^d	Hysteresis	Hysteresis + Néel + Brownian	Néel + Brownian	Brownian

^a Single domain diameter.

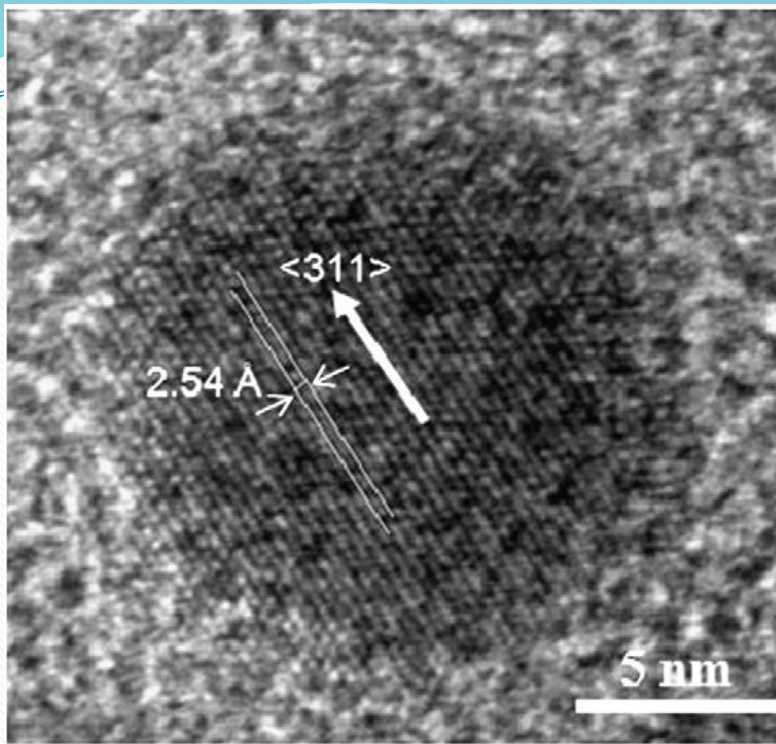
^b Superparamagnetic diameter.

^c In viscose medium.

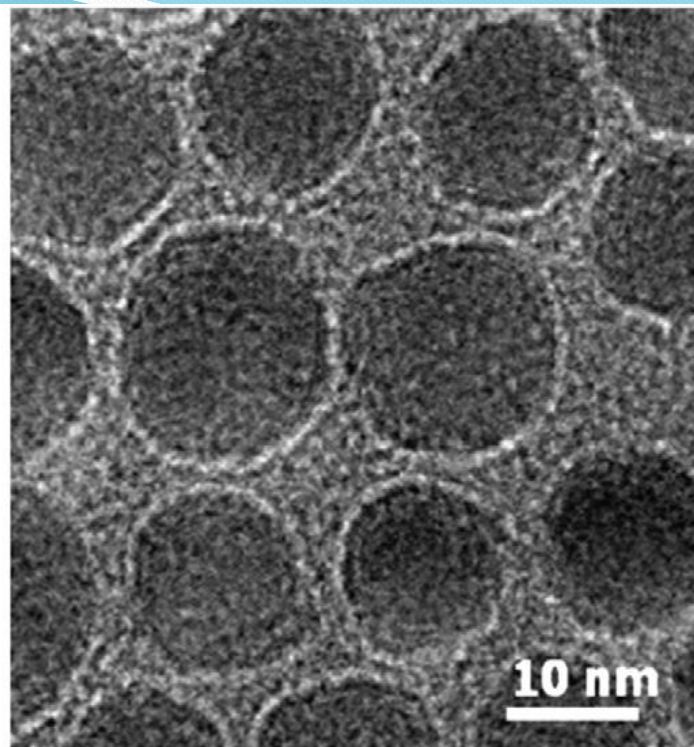
^d At high frequency and high magnetic field.

$$\tau_N = \tau_0 \exp(KV_M / k_B T)$$

$$\tau_B = \frac{3V_{hyd}}{k_B T} \eta$$



(a)

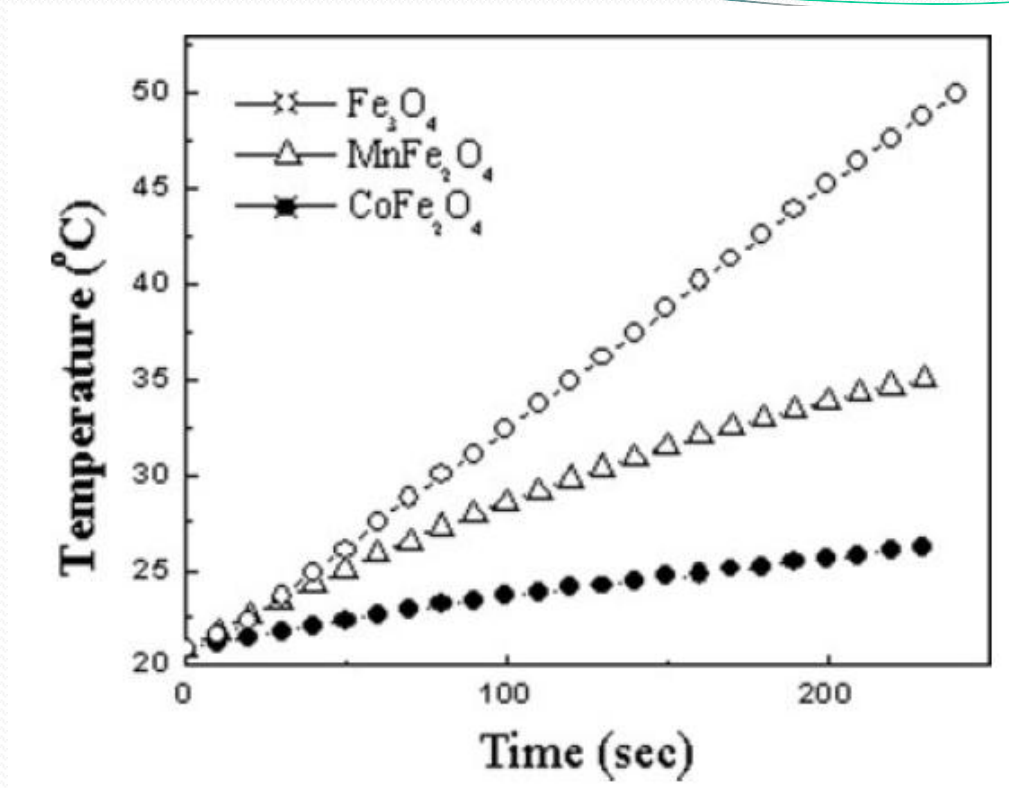


(b)

- TEM images of the synthesized (a) MnFe₂O₄ MNPs in high-resolution and (b) chitosan-MnFe₂O₄ MNPs

Magnetic compound	Core diameter (nm)	Corona	H (kA/m)	ν (kHz)	SAR (W/g _{Fe})	Author/group
Magnetite	13	Aminosilan	13	520	146	Jordan/Felix (1999)
Magnetite	18	Dextran	16	55	57	Li-Ying/Xu-Man (2007)
Magnetite	10	–	6.5	400	211 ^a	Hilger/Kaiser (2001)
Magnetite	9–10	Lauric acid	15	300	168	Bahadur (2006)
Manganese ferrite	10–11	Lauric acid	15	300	135.8	Bahadur (2006)
Manganese ferrite	10	Liposomes	15	300	135	Pradhan/Bahadur (2007)
Cobalt ferrite	6	Mercaptoundecanoic acid (11-MUA)	50	266	6 ^a	Dong-Hyun/Brazel (2008)
Cobalt ferrite	18	Suspended in gel of agarose	30	108	3.5 ^a	Veverka/Vasseur (2007)
Cobalt ferrite	9–10	Lauric acid	15	300	51.8	Bahadur (2006)
Cobalt ferrite	15	Lauric acid, dodecylamine, 1,2- hexadecanediol	5	300	396.1	Dravid (2009)

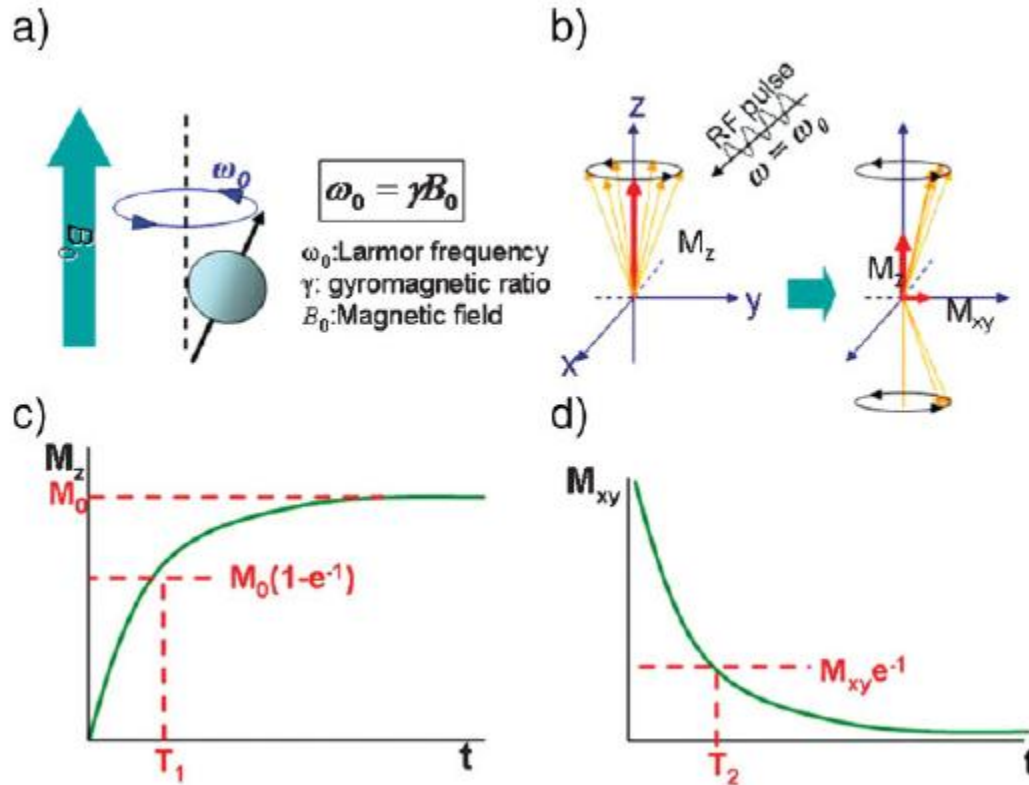
^a (W/g_{Ferrite}).



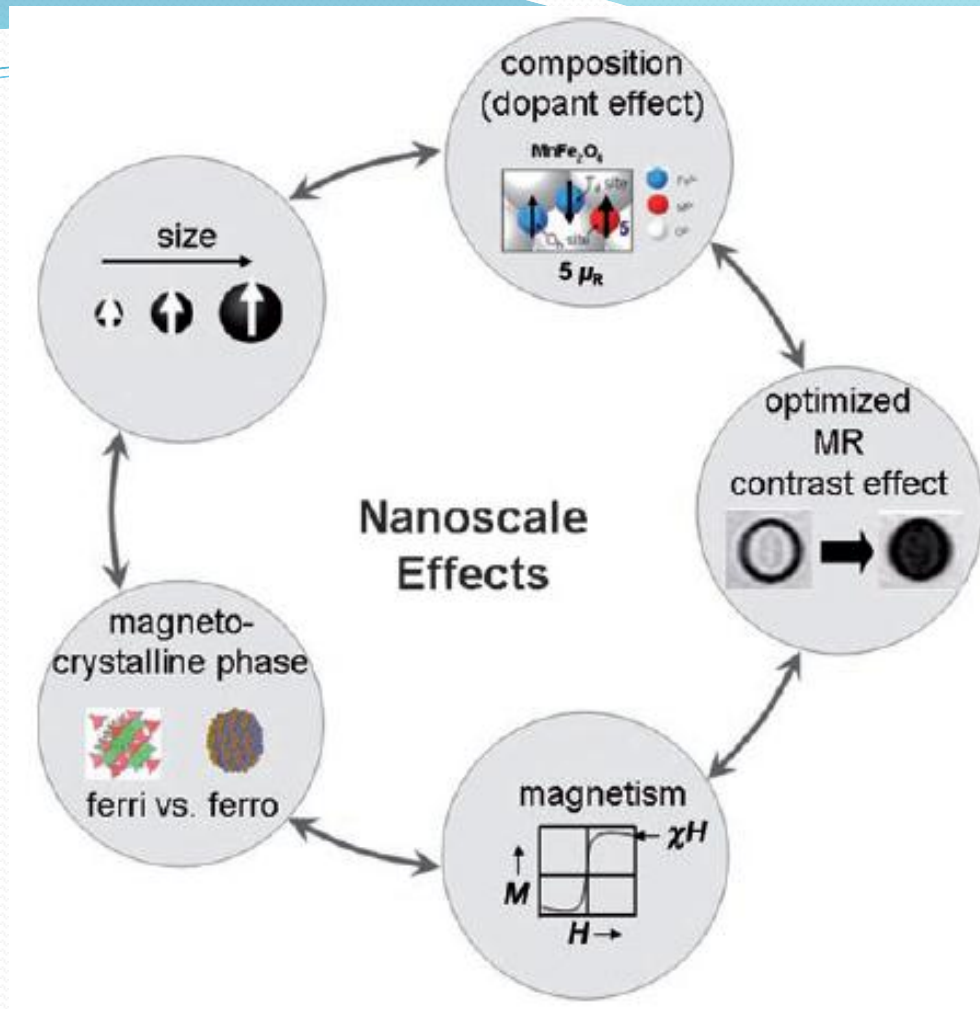
- Time-temperature curve of lauric acid-coated different
- ferrite-based magnetic fluids



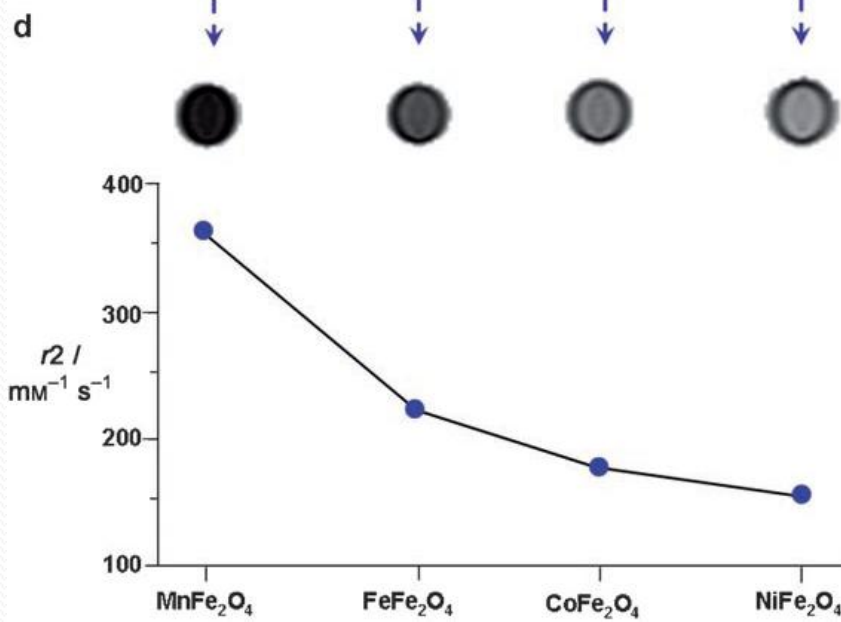
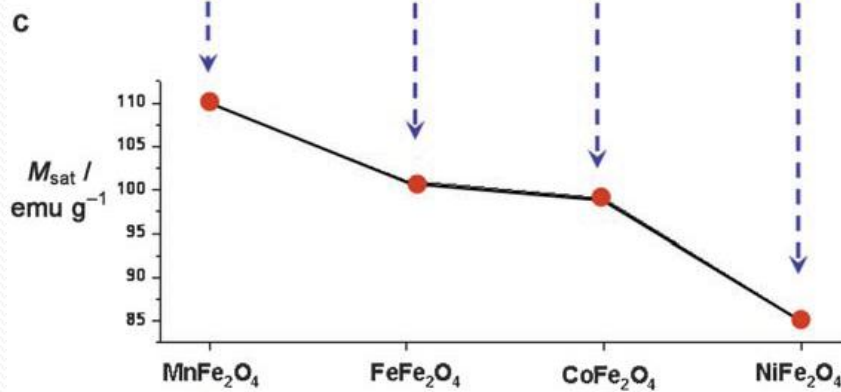
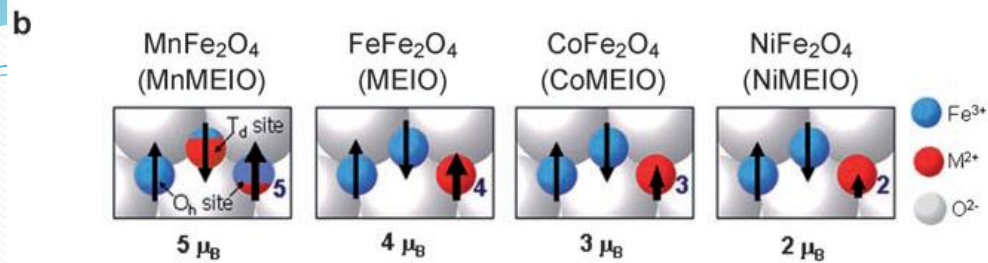
2. Magnetic Resonance Imaging (MRI)

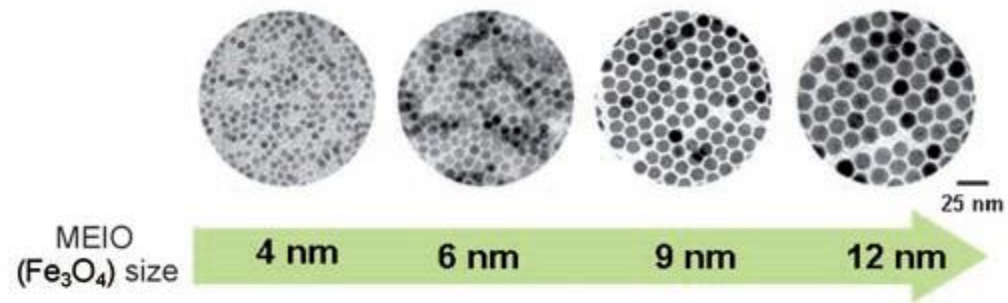
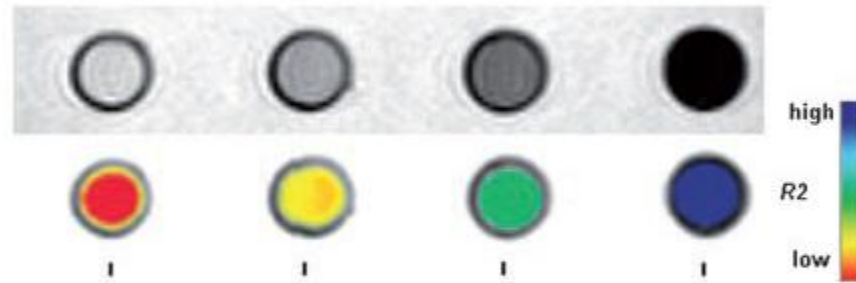
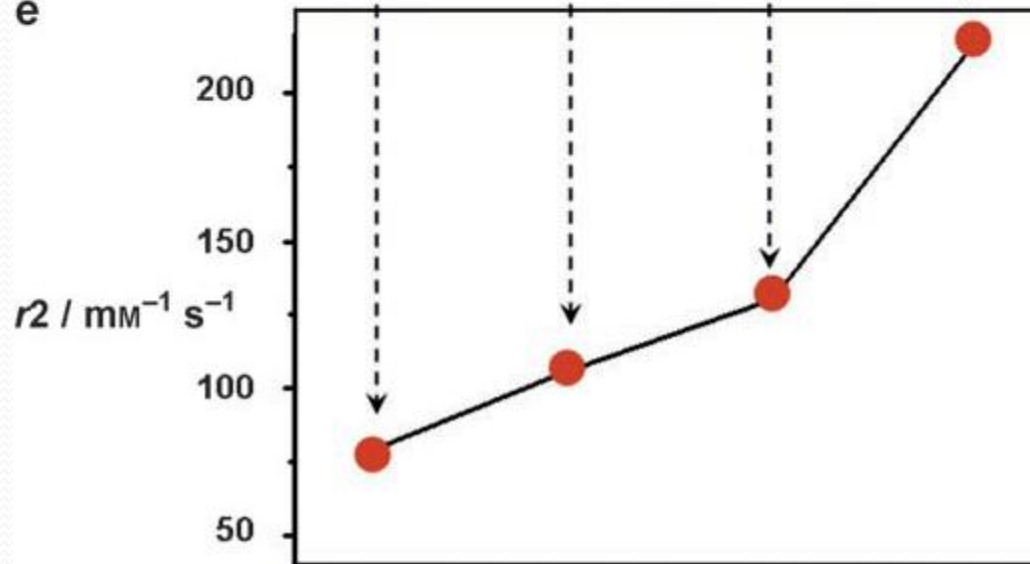


- Principle of magnetic resonance imaging. a) Spins align parallel or antiparallel to the magnetic field and precess under Larmor frequency (ω_0).
- b) After induction of RF pulse, magnetization of spins changes.
- Excited spins take relaxation process of c) T_1 relaxation and d) T_2 relaxation.



- Important parameters of MNPs for MR contrast-enhancement
 - effects.



b**c****d****e** Fe_3O_4

Name	Magnetic core size [nm]	Total size [nm]	Coating material	$r_2^{[a]}$ [$\text{mM}^{-1} \text{s}^{-1}$]	B [T]
<i>Conventional MNP Agents</i>					
AMI-25 (Feridex; Endorem) ^[51]	5–6	80–150	Dextran	ca. 100	0.47
SHU 555A (Resovist) ^[52]	ca. 4.2	ca. 62	Carbodextran	151	0.47
AMI-227 (Combidex; Sinerem) ^[53]	4–6	20–40	Dextran	53	0.47
CLIO; MION ^[54]	ca. 2.8	10–30	Dextran	ca. 69	1.5
<i>New Types of Synthetic MNPs</i>					
Fe_3O_4 (MEIO) ^[38]	12	15	DMSA	218	1.5
MnFe_2O_4 (MnMEIO) ^[38]	12	15	DMSA	358	1.5
FeCo ^[39]	7	30	Carbon and phospholipids-poly(ethylene glycol)	644	1.5

- The r_2 values are literature values and can be slightly variable depending on the field strength and MR pulse sequences

Name	Core Material	Surface	Diameter of Core [nm]	Hydrodynamic Diameter [nm]	Magnetization [emu g ⁻¹][a]	r_2 [mM ⁻¹ s ⁻¹]	B_0 [T]
Ferumoxides (Feridex)	Fe ₃ O ₄ , γ -Fe ₂ O ₃	Dextran	4.96	160	45	120	1.5
Ferucarbotran (Resovist)	Fe ₃ O ₄	Carboxydextran	4	60		186	1.5
Ferumoxtran (Combidex)	Fe ₃ O ₄	Dextran	5.85	35	61	65	1.5
CLIO-Tat	Fe ₃ O ₄	Dextran	5	30	60	62	1.5
WSIO (MEIO)	Fe ₃ O ₄	DMSA[b]	4		25	78	1.5
			6		43	106	
			9		80	130	
			12		101	218	
FeNP	α -Fe	PEG	10		70	129	1.5
MnMEIO	MnFe ₂ O ₄	DMSA[b]	6		68	208	1.5
			9		98	265	
			12		110	358	
CoMEIO	CoFe ₂ O ₄	DMSA[b]	12		99	172	1.5
NiMEIO	NiFe ₂ O ₄	DMSA[b]	12		85	152	1.5
Au-Fe ₃ O ₄	Fe ₃ O ₄	PEG	20			114	3.0
Au-FePt	FePt (fcc)	PEG	6			59	3.0

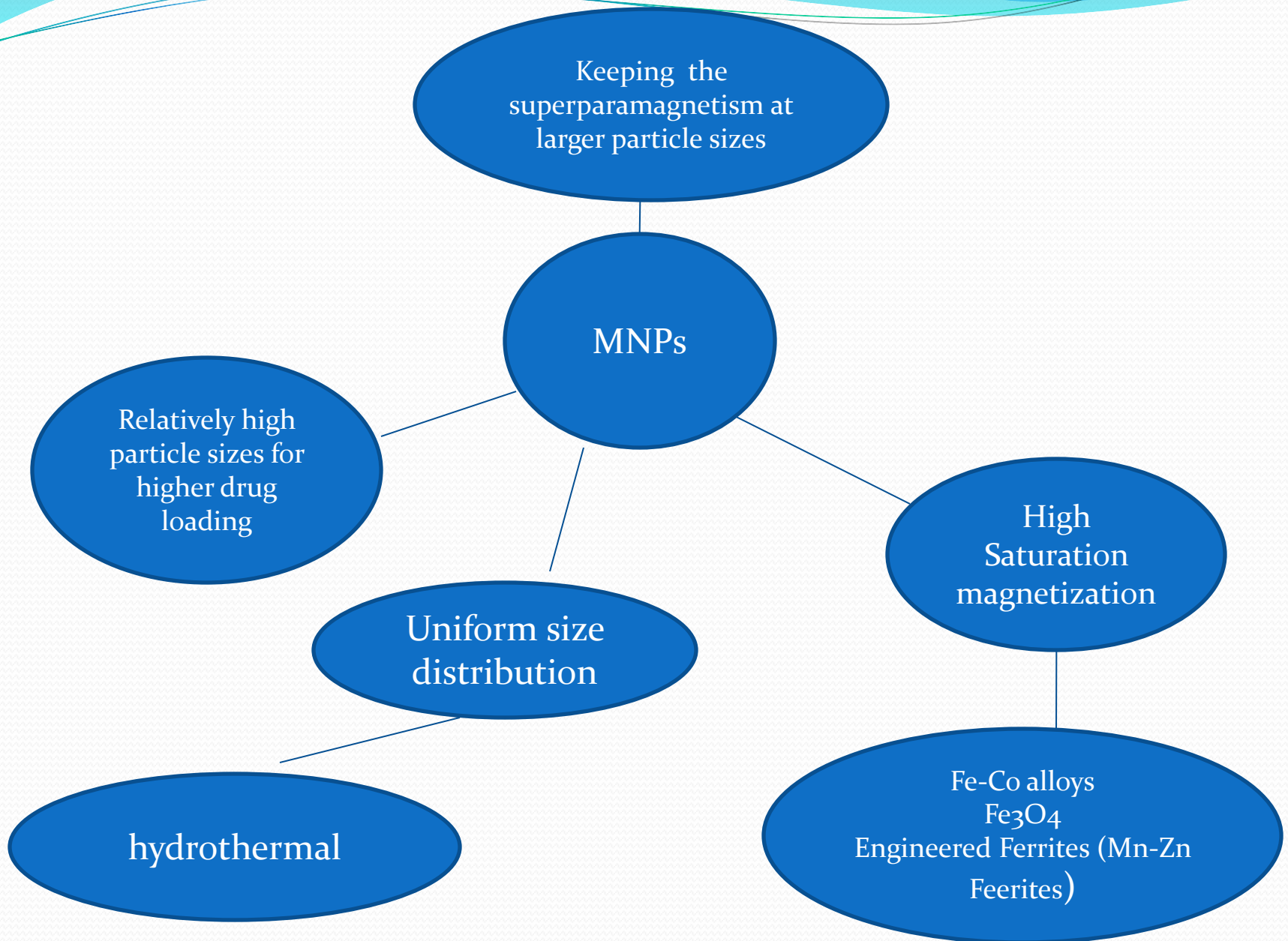
- Properties of T₂ contrast agents

Name	Core Material	Surface	Diameter of Core [nm]	Hydrodynamic Diameter [nm]
Dextran-SPGO	Gd ₂ O ₃	Dextran		26
PEG-Gd ₂ O ₃	Gd ₂ O ₃	PEG	3	
GadoSiPEG	Gd ₂ O ₃	Polysiloxane-PEG	2.2	3.3
			3.8	5.2
			4.6	8.9
GdF ₃ :cit	GdF ₃	Citric acid		129.3
GdF ₃ /LaF ₃ :AEP	GdF ₃ /LaF ₃	2-Aminoethyl Phosphate		51.5
PGP/dextran-K01	GdPO ₄	Dextran		23.2
MnO	MnO	PEG	7	
			15	
			20	
			25	
FeCo/GC	FeCo	Graphitic Carbon-PEG	4	30
			7	

- Properties of T₁ contrast agents based on inorganic nanoparticles

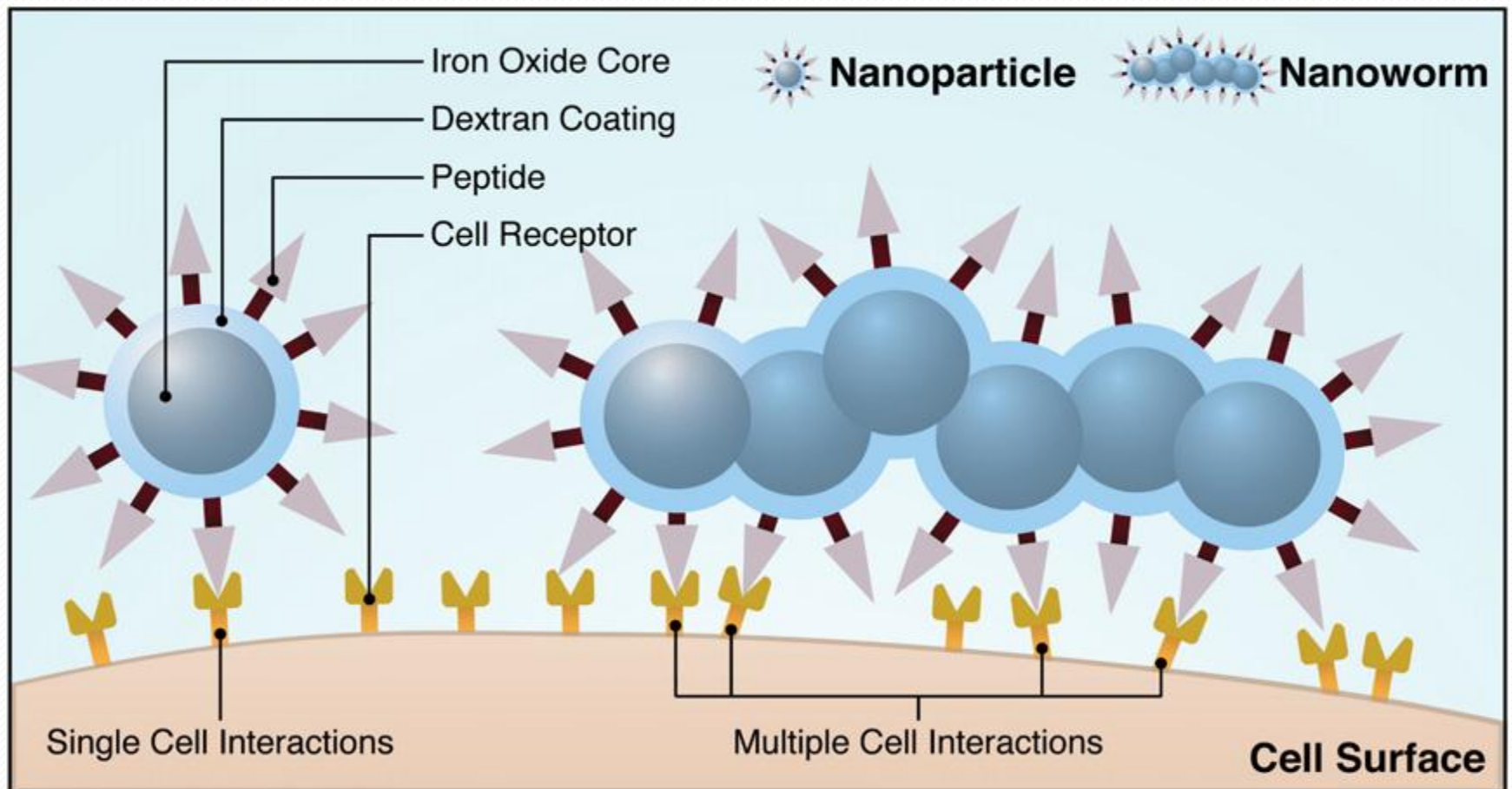
3. Drug Targeting

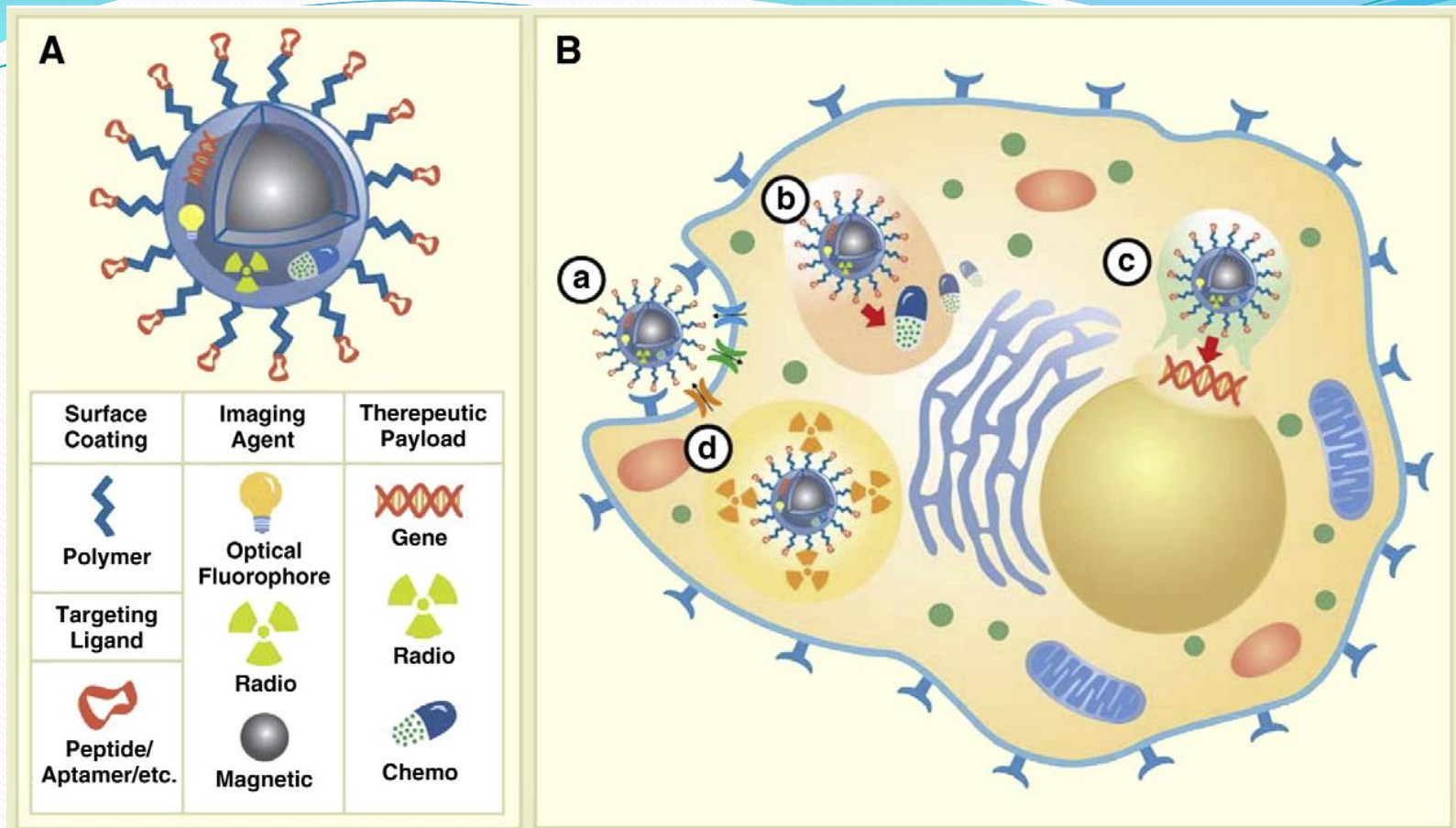
- The objectives are two-fold: (i) to reduce the amount of systemic distribution of the cytotoxic drug, thus reducing the associated side-effects; and (ii) to reduce the dosage required by more efficient, localized targeting of the drug.
- Once the drug/carrier is concentrated at the target, the drug can be released either via enzymatic activity or changes in physiological conditions such as pH, osmolality, or temperature, and be taken up by the tumour cells
-



- Fe/Fe₃O₄ nanoparticles were produced with a core radius of 4 nm and oxide thickness of 2.5 nm. Magnetic characterization of these MNPs confirmed that the particles were superparamagnetic and possessed a Ms of 102.6 emu/g Fe
- ✓ small NPs (<20 nm) are excreted renally
- ✓ medium sized NPs (30–150 nm) accumulated in the bone marrow ,heart, stomach
- ✓ large NPs (150–300 nm) have been found in the liver and spleen

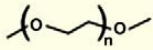
- Conceptual scheme illustrating the varying multivalent affinity interactions between receptors on a cell surface and targeting ligands on a nanospheres versus a nanoworm.



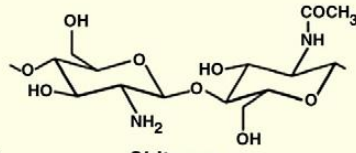


- Illustration of multifunctional imaging/therapeutic MNPs anatomy and potential mechanisms of action at the cellular level. (A) A multifunctional MNP modified with targeting ligands extended from MNP surface with polymeric extenders, imaging reporters (optical, radio, magnetic), and potential therapeutic payloads (gene, radio, chemo). (B) Four possible modes of action for various therapeutic agents; a) Specific MNP binding to cell surface receptors (i.e. enzymes/proteins) facilitate their internalization and/or inactivation, b) controlled intercellular release of chemotherapeutics; c) release of gene therapeutic materials post endosomal escape and subsequent targeting of nucleus; and d) intracellular decay of radioactive materials.

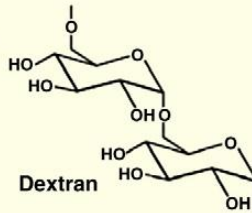
Coating Polymers



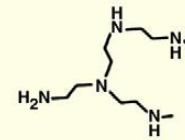
Poly(ethylene glycol) (PEG)



Chitosan



Dextran



Poly(ethylenimine) (PEI)

Polymer Types

End-grafted Polymers



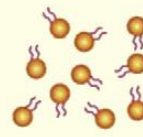
PEG

Surface Adsorption Polymers

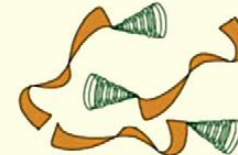


Chitosan, Dextran, PEI

Phospholipids



CoPolymers



PVA-PEG, Chitosan-PEG

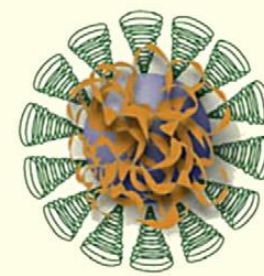
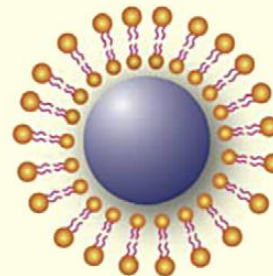
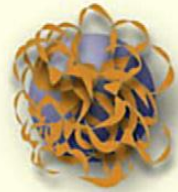
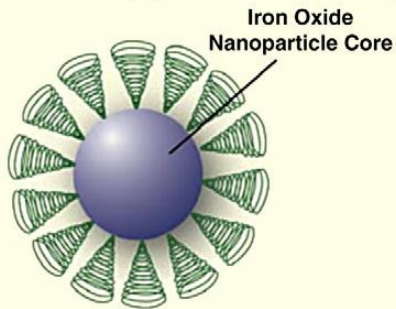
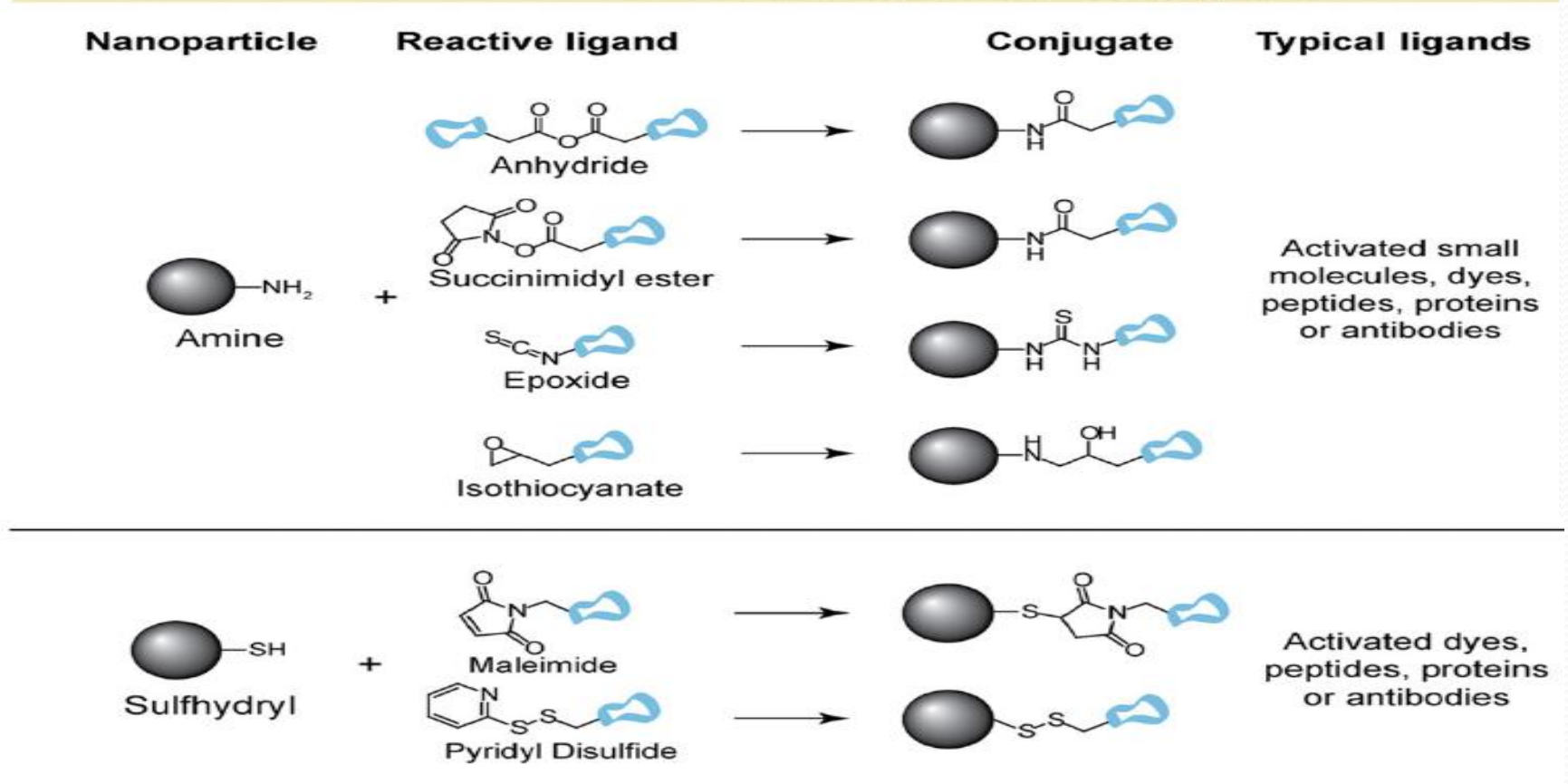



Illustration depicting the assembly of polymers onto the surface of magnetic nanoparticle cores.

Direct nanoparticle conjugation



- Examples of various SPION surface modification chemistry

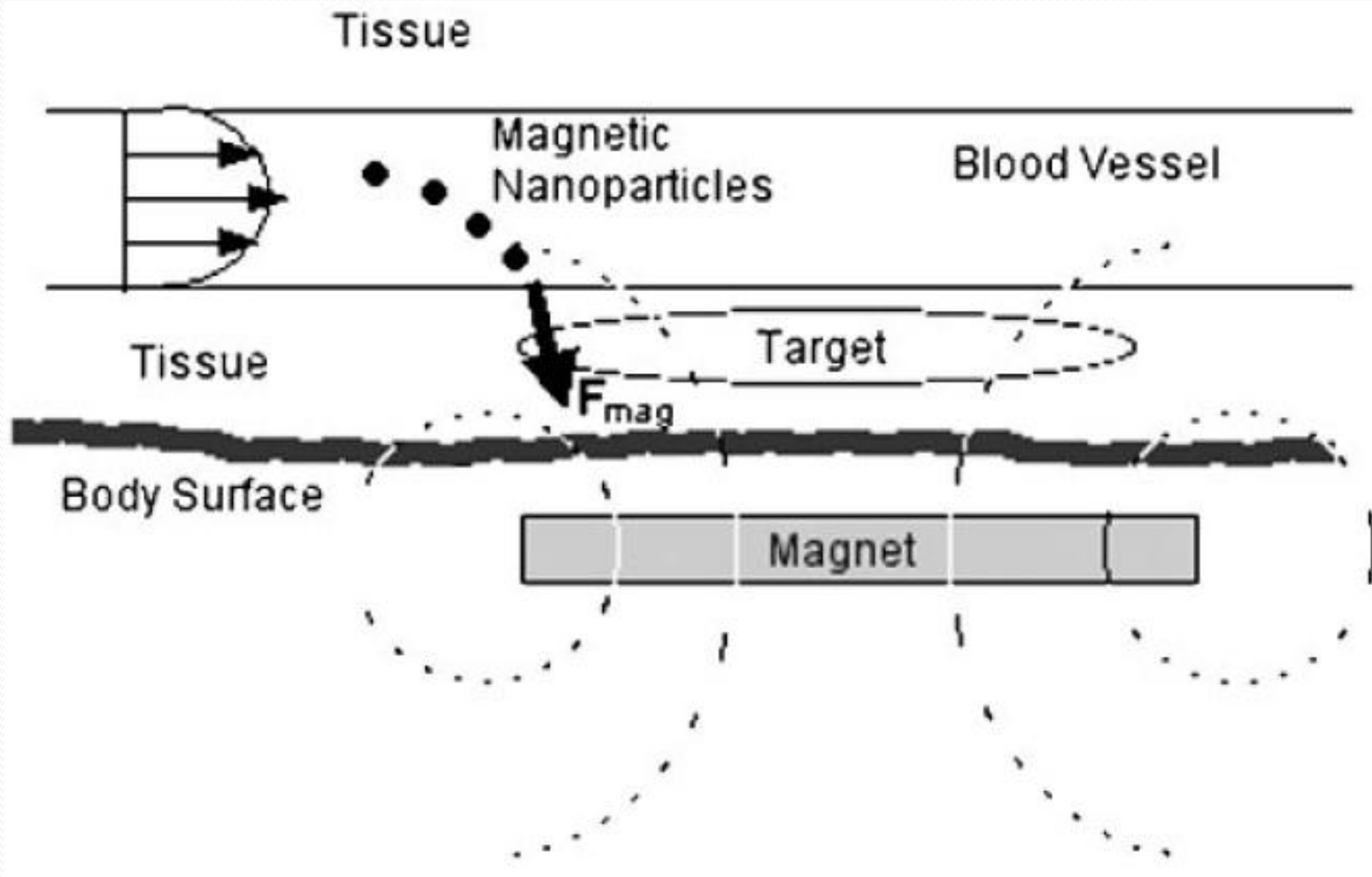
- NP biodistribution appears to be significantly influenced by its physicochemical properties. Hydrodynamic size, for instance, (1) helps govern the NP concentration profile in the blood vessel, (2) affects the mechanism of NP clearance, and (3) dictates the permeability of NPs out of the vasculature. In the case of the former, Decuzzi et al produced models suggesting that smaller sized, spherical NPs observed higher diffusion rates, increasing the NP concentration at the center of a blood vessel, thus limiting interactions with endothelial cells and prolonging the NP blood circulation time
- Hydrodynamic size also affects NP clearance from circulation . For instance, it has been reported that small NPs (<20 nm) are excreted renally, while medium sized NPs (30–150 nm) have accumulated in the bone marrow , heart, kidney and stomach, and large NPs (150–300 nm) have been found in the liver and spleen. While these size ranges provide general clearance mechanisms, other physical parameters simultaneously affect NP mobility.

- 
- ✓ Allowing the release of a drug over a prolonged period of time maximizes the effect of drugs such as chemotherapeutics that are effective only during a specific part of a cell's life cycle.
 - ✓ The drug may be released via degradation of the carrier particle or may be triggered by heat or pH

Magnetic targeting

- The magnetic targeting force must compete with the force due to linear blood-flow rates of about 0.05 cm/s in capillaries to 10 cm/s in arteries and 50 cm/s in the aorta.
- Iron-oxide nanoparticles require flux densities at the target site on the order of 0.1 to 1.0 T with field gradients ranging from 8 T/m (femoral arteries) to over 100 T/m for carotid arteries.

$$\vec{F}_m = (\vec{m} \cdot \vec{\nabla}) \vec{B}$$



- 
- organs such as the liver and the lungs are harder to target than organs closer to the surface or in the extremities.